16. Hayashi Y, Tsuji S, Tsujii M, Nishida T, Ishii S, Nakamura T, et al. The transdifferentiation of bone-marrow-derived cells in colonic mucosal regeneration after dextran-sulfate-sodium-induced colitis in mice. Pharmacology. 2007;80:193–9.
17. Jiang S, Walker L, Afentoulis M, Anderson DA, Jauron-Mills L, Corless CL, et al. Transplanted human bone marrow contributes to vascular endothelium. Proc Natl Acad Sci. 2004;101:16891–6.
18. Beck PL, Li Y, Wong J, Chen CW, Keenan CM, Sharkey KA, et al. Inducible nitric oxide synthase from bone marrow-derived cells plays a critical role in regulating colonic inflammation. Gastroenterology. 2007;132:1778–90.
19. Yabana T, Arimura Y, Tanaka H, Goto A, Hosokawa M, Nagaishi K, et al. Enhancing epithelial engraftment of rat mesenchymal stem cells restores epithelial barrier integrity. J Pathol. 2009;218:350–9.
20. Hayashi Y, Tsuji S, Tsuji M, Tsujii M, Nishida T, Iijima H, et al. Topical implantation of Mesenchymal stem cells has beneficial effects on healing of experimental colitis in rats. J Pharmacol Exp Ther. 2008;326:523–31.
21. Ando Y, Inaba M, Sakaguchi Y, Tsuda M, Quan GK, Omae M, et al. Subcutaneous Adipose tissue-derived stem cells facilitate colonic mucosal recovery from 2, 4, 6-trinitrobenzene sulfonic acid (TNBS)-induced colitis in rats. Inflamm Bowel Dis. 2008;14:826–38.
22. Khalil PN, Weiler V, Nelson PJ, Khalil MN, Moosmann S, Mutschler WE, et al. Nonmyeloablative stem cell therapy enhances microcirculation and tissue regeneration in murine inflammatory bowel disease. Gastroenterology. 2007;132:944–54.
23. Zhang Q, Shi S, Liu Y, Uyanne J, Shi Y, Le AD. Mesenchymal stem cells derived from human gingiva are capable of immunomodulatory functions and ameliorate inflammation-related tissue destruction in experimental colitis. J Immunol. 2009;183:7787–98.
24. Gonzalez-Rey E, Anderson P, González MA, Rico L, Buscher D, Delgado M. Human adult stem cells derived from adipose tissue protect against experimental colitis and sepsis. Gut. 2009;58:929–39.
25. Tanaka F, Tominaga K, Ochi M, Tanigawa T, Watanabe T, Fujiwara Y, et al. Exogenous administration of mesenchymal stem cells ameliorates dextran sulfate sodium-induced colitis via anti-inflammatory action in damaged tissue in rats. Life Sci. 2008;83:771–9.
26. Inoue H, Ohsawa I, Murakami T, Kimura A, Hakamata Y, Sato Y, et al. Development of new inbred transgenic strains of rats with LacZ or GFP. Biochem Biophys Res Commun. 2005;329:288–95.
27. Javazon EH, Colter DC, Schwarz EJ, Prockop DJ. Rat marrow stromal cells are more sensitive to plating density and expand more rapidly from single-cell-derived colonies than human marrow stromal cells. Stem Cells. 2001;19:219–25.
28. Romanov YA, Svintsitskaya VA, Smirnov VN. Searching for alternative sources of postnatal human mesenchymal stem cells: candidate MSC-Like cells from umbilical cord. Stem Cells. 2003;21:105–10.
29. Yoshiji H, Kuriyama S, Yoshii J, Ikenaka Y, Noguchi R, Nakatani T, et al. Angiotensin-II type 1 receptor interaction is a major regulator for liver fibrosis development in rats. Hepatology. 2001;34:745–50.
30. Iyonaga K, Takeya M, Yamamoto T, Ando M, Takahashi K. A novel monoclonal antibody, RM-4, specifically recognizes rat macrophages and dendritic cells in formalin-fixed, paraffin-embedded tissues. Histochem J. 1997;29:105–16.
31. Rieder F, Brenmoehl J, Leeb S, et al. Wound healing and fibrosis in intestinal disease. Gut. 2007;56:130–9.
32. Barnard JA, Beauchamp RD, Russell WE, Scholmerich J, Rogler G, et al. Epidermal growth factor-related peptides and their relevance to gastrointestinal pathophysiology. Gastroenterology. 1995;108:564–80.
33. Xian CJ, Cool JC, Howarth GS, Read LC. Effects of TGF-alpha gene knockout on epithelial cell kinetics and repair of methotrexate-induced damage in mouse small intestine. J Cell Physiol. 2002;191:105–15.
34. Yang Q, Bermingham NA, Finegold MJ, Zoghbi HY. Requirement of Math1 for secretory cell lineage commitment in the mouse intestine. Science. 2001;294:2155–8.
35. Okamoto R, Tsuchiya K, Nemoto Y, Akiyama J, Nakamura T, Kanai T, et al. Requirement of Notch activation during regeneration of the intestinal epithelia. Am J Physiol Gastrointest Liver Physiol. 2009;296:23–35.
36. González MA, Gonzalez-Rey E, Rico L, Buscher D, Delgado M. Adipose-derived mesenchymal stem cells alleviate experimental colitis by inhibiting inflammatory and autoimmune responses. Gastroenterology. 2009;136:978–89.
37. Wei Y, Nie Y, Lai J, Wan YJ, Li Y. Comparison of the population capacity of hematopoietic and mesenchymal stem cells in experimental colitis rat model. Transplantation. 2009;88:42–8.
38. Hilton MJ, Tu X, Wu X, Bai S, Zhao H, Kobayashi T, et al. Notch signaling maintains bone marrow mesenchymal progenitors by suppressing osteoblast differentiation. Nat Med. 2008;14:306–14.
39. Kinner B, Zaleskas JM, Spector M. Regulation of smooth muscle actin expression and contraction in adult human mesenchymal stem cells. Exp Cell Res. 2002;278:72–83.

DOI:10.1158/1940-6207.CAPR-10-0214

Research Article

Cancer Prevention Research

Epigenetic Alteration of DNA in Mucosal Wash Fluid Predicts Invasiveness of Colorectal Tumors

Seiko Kamimae[1], Eiichiro Yamamoto[1,2], Hiro-o Yamano[5], Masanori Nojima[3], Hiromu Suzuki[1,2], Masami Ashida[1], Tomo Hatahira[1], Akiko Sato[1], Tomoaki Kimura[5], Kenjiro Yoshikawa[5], Taku Harada[5], Seiko Hayashi[5], Hiroyuki Takamaru[2], Reo Maruyama[1,2], Masahiro Kai[1], Morie Nishiwaki[6], Tamotsu Sugai[7], Yasushi Sasaki[4], Takashi Tokino[4], Yasuhisa Shinomura[2], Kohzoh Imai[8], and Minoru Toyota[1]

Abstract

Although conventional colonoscopy is considered the gold standard for detecting colorectal tumors, accurate staging is often difficult because advanced histology may be present in small colorectal lesions. We collected DNA present in mucosal wash fluid from patients undergoing colonoscopy and then assessed the methylation levels of four genes frequently methylated in colorectal cancers to detect invasive tumors. We found that methylation levels in wash fluid were significantly higher in patients with invasive than those with noninvasive tumors. Cytologic and *K-ras* mutation analyses suggested that mucosal wash fluid from invasive tumors contained greater numbers of tumor cells than wash fluid from noninvasive tumors. Among the four genes, levels of *mir-34b/c* methylation had the greatest correlation with the invasion and showed the largest area under the receiver operating characteristic curve (AUC = 0.796). Using cutoff points of *mir-34b/c* methylation determined by efficiency considerations, the sensitivity/specificity were 0.861/0.657 for the 13.0% (high sensitivity) and 0.765/0.833 for the 17.8% (well-balanced) cutoffs. In the validation test set, the AUC was also very high (0.915), the sensitivity/specificity were 0.870/0.875 for 13.0% and 0.565/0.958 for 17.8%. Using the diagnostic tree constructed by an objective algorithm, the diagnostic accuracy of the invasiveness of colorectal cancer was 91.3% for the training set and 85.1% for the test set. Our results suggest that analysis of the methylation of DNA in mucosal wash fluid may be a good molecular marker for predicting the invasiveness of colorectal tumors. *Cancer Prev Res; 4(5); 674–83. ©2011 AACR.*

Introduction

Colorectal cancer is one of the most common neoplasias worldwide (1), and its early detection and accurate preoperative staging are essential for reducing the incidences of invasion and metastasis. The fecal occult blood test is widely used to screen for colorectal tumors, though its sensitivity and specificity are not high (2, 3). Conventional colonoscopy is considered the gold standard for detecting colorectal cancers and adenomas, whereas several other methods, including computed tomography, ultrasonography, and 3D magnetic resonance, have been used for staging (4, 5). Generally, tumor size is used as the marker for invasion and lymph node metastasis; however, accurate staging is often difficult because advanced histology may be present in as much as 10% of small (5–10 mm) colorectal adenomas (6–8).

Magnified endoscopy is a highly useful method for diagnosing invasive colorectal cancer (9, 10). Although conventional endoscopic examination with indigo carmine dye is not sufficient to determine whether or not a colorectal cancer is invasive, pit pattern analysis, using high-magnification observation with crystal violet, reportedly enables the diagnosis of invasive colorectal cancers. Recently, narrow-band imaging magnification endoscopy has also been used to predict the invasiveness of colorectal tumors (11). However, it has been suggested that the skills required for pit pattern analysis will limit the number of endoscopists who use the technique.

DNA methylation plays a critical role in the tumorigenesis of colorectal cancer (12, 13). For example, promoter hypermethylation is associated with the silencing of various cancer-related genes (14, 15), and aberrant methylation of the CpG islands of genes in stool and serum/plasma can be used as a molecular marker for detection of colorectal tumors (16–20). On the contrary, because DNA

Authors' Affiliations: [1]Department of Biochemistry, [2]First Department of Internal Medicine, [3]Department of Public Health, and [4]Department of Molecular Biology, Cancer Research Institute, Sapporo Medical University; [5]Akita Red Cross Hospital, Akita; [6]GeneticLab Co. Ltd., Sapporo; [7]Department of Pathology, Iwate Medical University, Morioka; and [8]The Institute of Medical Science, The University of Tokyo, Tokyo, Japan

Note: Supplementary data for this article are available at Cancer Prevention Research Online (http://cancerprevres.aacrjournals.org/).

S. Kamimae, E. Yamamoto, and H. Yamano contributed equally to this work.

Corresponding Author: Minoru Toyota, Department of Biochemistry, Sapporo Medical University, South-1, West-17, Chuo-ku, Sapporo 060-8556, Japan. Phone: 81-11-611-2111 (Ext. 2680); Fax: 81-11-622-1918. E-mail: mtoyota@sapmed.ac.jp

doi: 10.1158/1940-6207.CAPR-10-0214

DOI:10.1158/1940-6207.CAPR-10-0214

methylation is an early event (21–23), it does not enable one to distinguish between premalignant lesions and invasive tumors. As yet, there is no study describing a molecular test for predicting the invasiveness of colorectal tumors.

In this study, we examined the methylation levels of 4 genes frequently methylated in colorectal cancers by using DNA obtained from mucosal wash fluid. We found that the methylation level of DNA in the wash fluid was significantly higher in patients with invasive than those with noninvasive tumors. Our results suggest that methylation of DNA in mucosal wash fluid could be a good molecular marker for predicting the invasiveness of colorectal tumors.

Materials and Methods

Specimens and sample preparation

Colorectal tumor tissues and washing fluid were collected from Japanese patients who underwent endoscopic mucosal resection (EMR) or surgical resection of colorectal tumors at Akita Red Cross Hospital. Informed consent was obtained from all patients before collection of the specimens. Approval for this study was obtained from the Institutional Review Board of Akita Red Cross Hospital and Sapporo Medical University.

We used 2 methods to obtain DNA from mucosal washing fluid. When a colorectal tumor was detected during colonoscopy, the tumor's surface mucus was either washed away by using 20 mL of water, which was aspirated through the suction channel of the endoscope, and suspended in ThinPrep PreservCyt solution (Hologic, Inc.; method 1) or washed away with 20 mL of normal saline by using an NT tube and collected (method 2). Each sample of collected washing fluid was placed in a Non-GYN PreservCyt vial (Hologic, Inc.) for a minimum of 15 minutes, after which the solution was transferred to a disposable centrifuge tube and centrifuged at 500 × *g* for 20 minutes. The resultant supernatant was discarded, and the cell pellet was suspended in ThinPrep solution until DNA extraction. After collection of the washing fluid and endoscopic observation, biopsies of the colorectal tumor and corresponding normal colonic mucosa were carried out by using biopsy forceps under endoscopic guidance. For cytology analysis, a ThinPrep slide was prepared by a T2000 ThinPrep processor (Hologic, Inc.) and a nongynecologic ThinPrep Filter with 5-μm pores. The slide was then Papanicolaou stained and examined by GLab cytotechnologists and a pathologist (GeneticLab Co. Ltd.), and atypical cells were identified. Nuclei were stained by 4′,6-diamidino-2-phenylindole (DAPI) and visualized under a fluorescence microscope (Olympus) as described previously (24).

A total of 337 biopsy specimens including 150 colorectal tumors and 187 normal colonic mucosa specimens were examined. We also examined 88 samples of washing fluid from 70 colorectal tumor patients and 18 healthy patients. For testing the clinical usefulness of the study, we examined an additional 47 colorectal tumor biopsy samples as the test set, which were independently obtained several months after the collection of prior samples. On the basis of histologic examination after any type of resection, biopsy specimens and wash fluid samples from a colorectal tumor were divided into 2 groups: invasive tumors and noninvasive tumors. Invasive tumors were defined as submucosal invasive tumors.

Bisulfite pyrosequencing

DNA was extracted from biopsy specimens and washing fluid by using the standard phenol-chloroform procedure, after which 1-μg samples of genomic DNA were modified with sodium bisulfite by an EpiTect Bisulfite Kit (Qiagen). Bisulfite pyrosequencing was then carried out as described previously (25). Primers for pyrosequencing were designed by PSQ Assay Design software (Qiagen). Following PCR, the biotinylated PCR product was purified, made single-stranded, and then used as a template in a pyrosequencing reaction run according to the manufacturer's instructions. The PCR products were bound to streptavidin Sepharose beads HP (Amersham Biosciences), after which beads with the immobilized PCR product were purified, washed, and denatured by using a 0.2 mol/L NaOH solution. After addition of 0.3 μmol/L sequencing primer to the purified PCR product, pyrosequencing was carried out by a PSQ96MA system (Qiagen) and Pyro Q-CpG software (Qiagen). The primer sequences are listed in Supplementary Table S1.

K-ras mutation analysis

Mutation of codons 12 and 13 of *K-ras* was examined by using direct sequencing and pyrosequencing, as described previously (26). Pyrosequencing was done by a *K-ras* mutation detection kit (Qiagen) as suggested by the supplier.

Statistical analysis

All statistical analyses were carried out by SPSSJ 15.0 (SPSS Japan Inc.). To compare differences in methylation levels or other continuous values between groups, *t* tests or ANOVA with a post hoc Tukey test were carried out. Fisher's exact test was used for analysis of categorical data. To evaluate correlations between continuous values, Pearson's correlation coefficients were calculated. Receiver operating characteristic (ROC) curves for the diagnosis of invasive tumors were constructed on the basis of methylation levels, followed by area under the curve (AUC) calculation. A diagnostic tree to discriminate invasive tumors was constructed by using the training set based on the following objective algorithm. Step 1: classify the samples based on the most efficient cutoff of tumor size. Step 2: classify the samples based on the most efficient cutoffs of methylation levels in 4 sequences under the classification of the previous step. Step 3: repeat step 2 until no additional efficacy is observed. $P < 0.05$ (2-sided) were considered significant.

Results

Preparation of specimens

We first compared the 2 methods used to obtain tumor cells from colonoscopy wash fluid. When tumors were

DOI:10.1158/1940-6207.CAPR-10-0214

Table 1. Amounts of DNA and quality of cytology obtained by using the 2 collection methods tested

	Biopsy (n = 11)	Wash fluid (method 1)			Biopsy (n = 37)	Wash fluid (method 2)		
		Total (n = 11)	IT (n = 8)	NI (n = 3)		Total (n = 37)	IT (n = 18)	NI (n = 19)
DNA, μg	21.28 ± 15.25	15.00 ± 11.12			17.08 ± 13.00	16.53 ± 16.88		
Cytology								
Diagnosable		2	1	1		17	11	6
Not diagnosable		9	7	2		20	7	13
		18.2%	12.5%	33.3%		45.9%	61.1%	31.6%

Abbreviations: IT: invasive tumors, NI: noninvasive tumors.

found during colonoscopy, the tumor surfaces were washed with water (method 1) or saline (method 2; Supplementary Fig. S1A and B). Both methods enabled us to obtain enough DNA for molecular analysis (Table 1), but comparison of the cytology revealed that wash fluid obtained with saline (method 2) enabled more accurate detection of anaplastic cells (Supplementary Fig. S1B; Supplementary Table 1). We therefore used method 2 for subsequent analyses.

DNA methylation in biopsy specimens

The clinical features of the patients examined in this study are summarized in Table 2. There was no statistically significant difference in age or gender between patients with invasive and noninvasive tumors. We selected 4 genes for analysis, *mir-34b/c*, *SFRP1*, *SFRP2*, and *DKK2*, which are frequently methylated in colorectal cancer (25, 27, 28). Methylation analysis was carried out by using bisulfite pyrosequencing with DNA from 337 specimens, including 52 invasive tumors, 98 noninvasive tumors, and 187 specimens of normal colon tissue. We found that the methylation levels of the 4 genes were significantly higher in cancerous tissue than in normal colorectal mucosa (Fig. 1); however, we found no difference in tissue methylation levels between invasive and noninvasive tumors.

DNA methylation in mucosal washing fluid

We next examined gene methylation in 76 samples of mucosal wash fluid from 36 patients with invasive tumors and 34 with noninvasive tumors, and from 18 patients without colorectal lesions (Fig. 1). When we compared the invasive and noninvasive tumors, we found no differences for *SFRP2* and *DKK2*. However, *mir-34b/c* and *SFRP1* showed higher levels of methylation in wash fluid from patients with invasive than with noninvasive tumors.

We then used ROC analysis to further compare mucosal wash fluid from invasive and noninvasive tumors (Fig. 3A and B). The odds ratios (OR) for the risk of invasion associated with the methylation levels of the 4 genes tested are shown in Table 3. High levels of methylation were significantly associated with an increased risk of invasion. Among the 4 genes, levels of *mir-34b/c* methylation had the greatest impact on the risk of invasion and showed the largest AUC (0.796). Using various cutoff points of *mir-34b/c* methylation determined on the basis of efficiency considerations for clinical use, the sensitivity/specificity were 0.861/0.657 for the 13.0% (high sensitivity) cutoff point and 0.765/0.833 for the 17.8% (well balanced) cutoff. We also subdivided the tumors on the basis of whether they were ≥25 mm or <25 mm in size. In tumors 25 mm or larger, *mir-34b/c* showed the highest AUC (0.816); its sensitivity/specificity was 0.862/0.667 and its OR was 12.5. In tumors smaller than 25 mm, *SFRP1* showed the highest AUC (0.810), with a sensitivity/specificity of 0.821/0.833 and an OR of 23.0.

We further verified the utility of DNA methylation in mucosal washing, using an independent set of specimens, which was established as the test set (Figs. 2, 3C and D; Table 4). All of these ROC analyses were considered the training set. In the test set, the methylation levels of *mir-34b/c* showed very high AUC again (0.915), sensitivity/specificity was 0.870/0.875 for the 13.0% cutoff, and 0.565/0.958 for the 17.8% cutoff. In tumors 25 mm or larger, the AUC of the methylation levels of *mir-34b/c* was 0.778. In tumors smaller than 25 mm, the AUC of the methylation levels of *SFRP1* was 0.695.

To make a more efficient diagnostic method suitable for clinical situations, we then constructed a diagnostic tree to classify invasive and noninvasive tumors on the basis of the combination of methylation levels detected in wash fluid (Fig. 4A). First, because most endoscopists make an endoscopic diagnosis according to the size of lesions, we defined the most efficient cutoff of tumor size as the first node of the diagnostic tree. As the next nodes, we used the most efficient cutoffs of the methylation levels of the 4 genes (*mir-34*, *SFRP1*, *SFRP2*, and *DKK2*). For example, as shown in Figure 4A, if the tumor size is more than 25 mm and the methylation level of *mir-34b/c* is more than 15%, this lesion is diagnosed as an invasive tumor. In the training set, the sensitivity and specificity were 0.943 (33/35) and 0.882 (30/34), respectively. The total accuracy of the diagnosis was 91.3% (63/69). For use in clinical situations, we validated this diagnostic tree by using an independent test set (n = 47). The application of the diagnostic tree to the test set is shown in Figure 4B. Although a slight reduction in

DOI:10.1158/1940-6207.CAPR-10-0214

Table 2. Clinicopathologic features of the patients

	Training set								Test set					
	Biopsy sample				Washing fluid				Biopsy sample			Washing fluid		
	IT (n = 52)	NI (n = 98)	P	Normal (n = 187)	IT (n = 36)	NI (n = 34)	P	Normal (n = 18)	IT (n = 20)	NI (n = 21)	P	IT (n = 23)	NI (n = 24)	P
Demographics														
Age	67.4	66.7	0.720	67.2	68.8	64.7	0.101	59.6	69.3	69.6	0.553	70.3	69.3	0.707
Male	16 (30.8%)	24 (24.5%)		126 (67.4%)	22 (61.1%)	25 (73.5%)		9 (50.0%)	14 (70%)	14 (66.7%)		14 (60.9%)	17 (70.8%)	
Female	36 (69.2%)	74 (75.5%)	0.408	61 (32.6%)	14 (38.9%)	9 (26.5%)	0.269	9 (50.0%)	6 (30%)	7 (33.3%)	0.332	9 (39.1%)	7 (29.2%)	0.213
Tumor size														
≥25 mm	31 (59.6%)	12 (12.2%)			27 (75%)	5 (14.7%)			15 (75%)	3 (14.3%)		18 (78.3%)	3 (12.5%)	
<25 mm	21 (40.4%)	86 (87.8%)	<0.001		9 (25%)	29 (85.3%)	<0.001		5 (25%)	18 (85.7%)	<0.001	5 (21.7%)	21 (87.5%)	<0.001
Location														
Right	21 (40.4%)	44 (44.9%)			12 (33.3%)	17 (50%)			11 (55%)	12 (57.1%)		11 (47.8%)	13 (54.2%)	
Left	15 (28.8%)	25 (25.5%)			14 (38.9%)	7 (20.6%)			7 (35%)	7 (33.3%)		8 (34.8%)	8 (33.3%)	
Rectum	16 (30.8%)	29 (29.6%)	0.853		10 (27.8%)	10 (29.4%)	0.332		2 (10%)	2 (9.5%)	0.883	4 (17.4%)	3 (12.5%)	0.980
Histology														
Hyper/inflammatory		15 (15.3%)				3 (8.8%)				0 (0.0%)			0 (0.0%)	
Tubular adenoma		29 (29.6%)				10 (29.4%)				9 (42.9%)			12 (50%)	
Tubulovillous adenoma		28 (28.6%)				7 (20.6%)				7 (33.3%)			7 (29.2%)	
Severe dysplasia		26 (26.5%)				14 (41.2%)				5 (23.8%)			5 (20.8%)	
Cancer	52 (100.0%)				36 (100.0%)				20 (100.0%)			23 (100.0%)		

Abbreviations: IT: invasive tumors, NI: noninvasive tumors.

DOI:10.1158/1940-6207.CAPR-10-0214

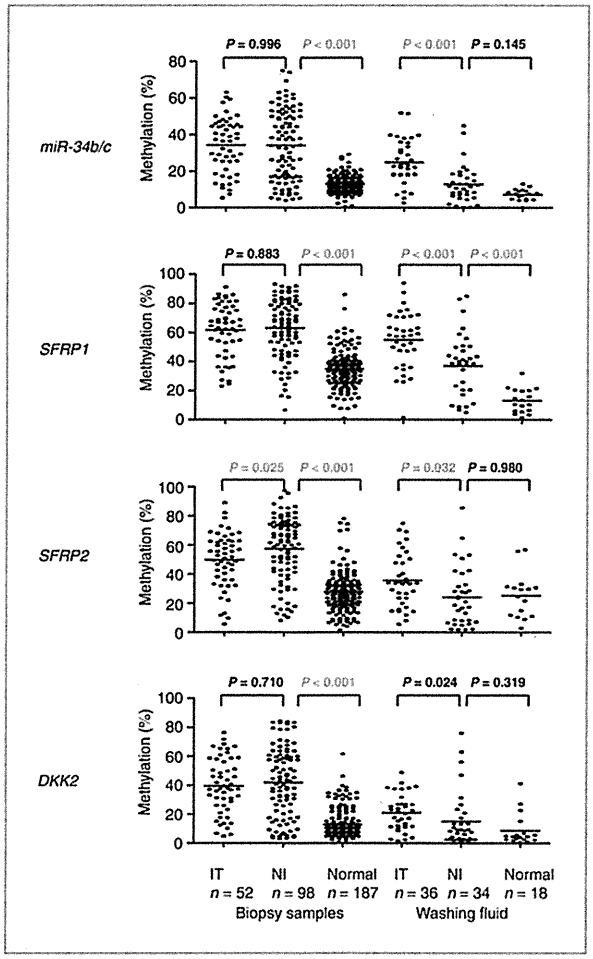

Figure 1. Levels of *mir-34b/c*, *SFRP1*, *SFRP2*, and *DKK2* methylation in invasive and noninvasive colorectal tumors. Methylation levels detected with DNA from biopsy and wash fluid. The genes analyzed are shown on the left.

sensitivity was observed (0.740, 17/23), the specificity was very high (0.958, 21/24). The total accuracy of the diagnosis was 85.1% (40/47) for the test set.

We also assessed the correlation between methylation levels detected in biopsy specimens and in wash fluid (Supplementary Fig. S2). We found that overall methylation levels in biopsy tissues and washing fluid were well correlated. When we divided the data for invasive and noninvasive tumors, however, only invasive tumors showed a significant correlation between methylation levels in biopsy tissue and washing fluid.

Detection of *K-ras* mutation by mucosal washing fluid

Finally, we tested for mutation of *K-ras* codons 12 and 13 by using DNA obtained from biopsy tissue or wash fluid (Supplementary Table S2). With invasive tumors, mutations of *K-ras* were found in 9 of 27 (33.3%) biopsy specimens. Among the 9 positive tumors, we were able to also detect mutations in 7 (77.7%) wash fluid samples. With noninvasive tumors, mutations were detected in 6 of 24 (25%) biopsy specimens, but in only 2 (33.3%) of the corresponding wash fluid samples. Addition of *K-ras* mutation did not improve the accuracy of diagnosis of invasiveness by the diagnostic tree (data not shown). Consistent with this finding, nuclear staining showed more intact nuclei in wash fluid from invasive tumors than from noninvasive tumors (Supplementary Fig. S1C). Thus, samples from invasive tumors seem to contain higher concentrations of tumor-derived DNA than samples from noninvasive tumors.

Discussion

Small colorectal tumors are usually removed by endoscopic mucosal dissection, but if the tumor is invasive, surgical treatment is required because of the higher risk of lymph node metastasis. Consequently, precise preoperative diagnosis is critical for appropriate treatment of colorectal tumors. Magnifying colonoscopy is a useful means of distinguishing invasive from noninvasive tumors (9, 10).

Table 3. Results of ROC analyses of the methylation levels in 4 genes in the training set.

Tumor size	Training set					
	Genes	AUC Estimate (95% CI)	Cutoff (%)	Sensitivity Estimate (95% CI)	Specificity Estimate (95% CI)	ORs Estimate (95% CI)
Total	*miR34b/c*	0.796 (0.686–0.906)	13.0	0.861 (0.705–0.953)	0.647 (0.465–0.803)	11.4 (3.5–36.9)
			17.8	0.833 (0.609–0.899)	0.765 (0.588–0.893)	16.3 (5.0–53.0)
			21.0	0.611 (0.435–0.769)	0.882 (0.726–0.967)	11.8 (3.4–40.7)
	SFRP1	0.736 (0.616–0.857)	45.0	0.750 (0.578–0.879)	0.706 (0.525–0.849)	7.2 (2.5–20.7)
	SFRP2	0.688 (0.562–0.814)	33.0	0.583 (0.408–0.745)	0.765 (0.588–0.893)	4.5 (1.6–12.8)
	DKK2	0.702 (0.572–0.831)	11.0	0.806 (0.64–0.918)	0.647 (0.465–0.803)	7.6 (2.6–22.5)
≥25mm	*miR34b/c*	0.816 (0.665–0.967)	15.0	0.862 (0.683–0.961)	0.667 (0.223–0.957)	12.5 (1.7–92.3)
<25mm	*SFRP1*	0.810 (0.594–1.000)	51.0	0.821 (0.631–0.939)	0.833 (0.359–0.996)	23.0 (2.2–242.1)

DOI:10.1158/1940-6207.CAPR-10-0214

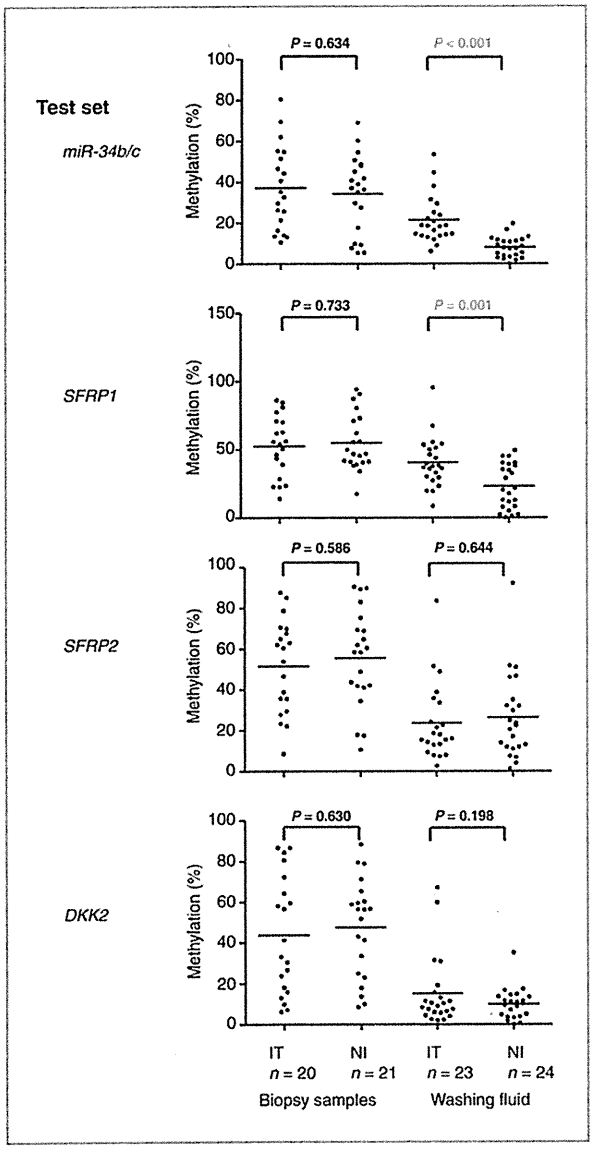

Figure 2. Methylation levels of *mir-34b/c*, *SFRP1*, *SFRP2*, and *DKK2* in the test set. Methylation levels detected with DNA from biopsy tissues and wash fluid. The genes analyzed are shown on the left.

However, invasive colorectal tumors show a heterogeneous pit pattern, making it difficult to determine a therapeutic strategy based on pit pattern diagnosis alone (29). Notably, surface mucus is washed away during magnifying endoscopic analysis, so that utilization of the wash fluid could be an effective noninvasive approach to diagnosis. It has been recommended that nearly all colorectal cancer patients who receive EMR receive periodic endoscopy for early detection of relapses (30). Examination of the methylation levels in the wash fluid could provide helpful information as to how often the patient should receive the follow-up endoscopy (e.g., the lower the methylation level, the less frequently endoscopic examination may be needed). In addition, although we did not include follow-up in our study, it is possible that wash fluid analysis could help physicians detect mucosal relapse after EMR during follow-up endoscopy.

It has been reported that DNA methylation in wash fluid containing pancreatic juice, saliva, or gastric juice is useful for diagnosis and risk assessment in cancer (34–36). For example, Watanabe and colleagues reported that DNA methylation in gastric wash fluid is useful for detection of early gastric cancer (36). The unique feature of our study is that it suggests DNA methylation in colon mucosal wash fluid can be used to predict the invasiveness of tumors. Further study will be necessary to determine whether DNA methylation of colon mucosal wash might also be useful for screening or risk assessment in cancer.

Here we showed that levels of *mir-34b/c* gene methylation were predictive of the invasiveness of colorectal tumors (Figs. 3 and 4; Tables 3 and 4). The sensitivity (0.833) and specificity (0.765) of this approach (well balanced cutoff), as well as the ROC AUC value (0.796), suggest methylation of this gene in colonoscopic wash fluid is a good molecular marker that distinguishes invasive from noninvasive colorectal tumors. We also showed that a diagnostic tree constructed by the combination of methylation levels was highly accurate for predicting invasiveness. To avoid unneeded surgery, it is important that the prediction of invasiveness is highly specific. In this regard, the specificities of the diagnostic tree were 0.882 in the training set, and 0.958 in the test set.

There is currently no molecular test that distinguishes invasive from noninvasive colorectal tumors. DNA methylation can be used as a biomarker for detection of colorectal lesions (16–20), but genes frequently methylated in cancer are also frequently methylated in early lesions (e.g., adenomas), and even in normal colorectal mucosa from aged patients (21, 22). It is therefore difficult to distinguish invasive tumors from noninvasive ones. We previously showed that *SFRP1* and *SFRP2* are frequently methylated in colorectal cancer (28). However, they are also often methylated in normal colorectal mucosa in an age-related manner (34), which is consistent with our present findings. The *mir-34b/c* gene is a putative tumor suppressor whose expression is induced by p53 (35). We previously showed that *mir-34b/c* is silenced by DNA methylation in colorectal cancers and adenomas (25). In this study, we found that methylation of *mir-34b/c* in noninvasive tumors is as high as that in invasive tumors. By contrast, levels of *mir-34b/c* methylation in normal colorectal mucosa are low. Thus, given the high frequency of methylation in tumors, tumor-specific methylation of *mir-34b/c* may be a highly useful molecular marker for colorectal cancer.

The molecular mechanism underlying the high levels of DNA methylation in wash fluid from invasive tumors is not fully understood. Analysis of nuclear staining, DNA methylation, and *K-ras* mutation suggest that wash fluid–derived DNA from invasive tumors contains higher concentrations of tumor-derived DNA than wash fluid from

DOI:10.1158/1940-6207.CAPR-10-0214

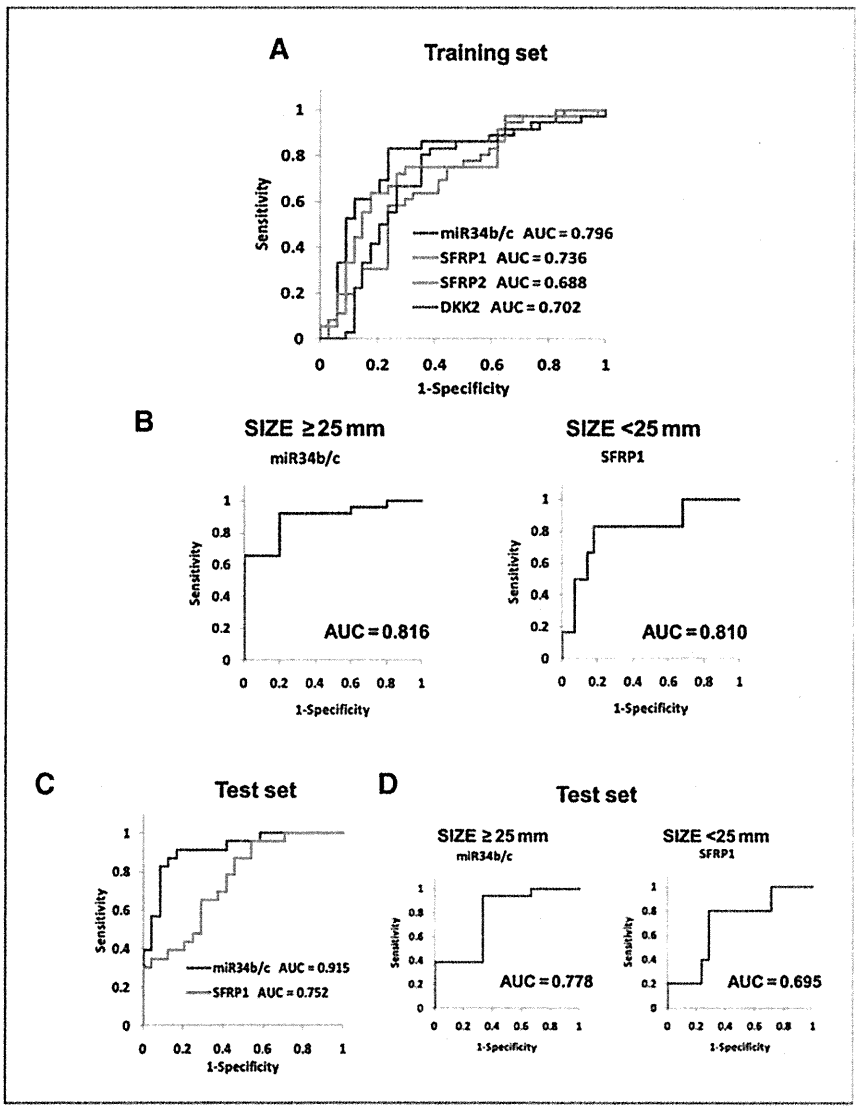

Figure 3. ROC curve analysis. ROC curves were constructed by plotting sensitivity vs. 1-specificity. Curves are shown comparing invasive vs. noninvasive tumors. AUCs are also shown in the graphs. A and B, ROC curve analysis for the training set. Overall analysis is shown in A, and stratified analysis by tumor size (≥25 mm or <25 mm) is shown in B. C and D, the same analysis for the test set. Overall analysis is shown in C, and that stratified by tumor size (≥25 mm or <25 mm) is shown in D.

Table 4. Results of ROC analyses of the methylation levels in 4 genes in the test set.

		Test set				
Tumor size	Genes	AUC Estimate (95% CI)	Cutoff (%)	Sensitivity Estimate (95% CI)	Specificity Estimate (95% CI)	ORs Estimate (95% CI)
Total	*miR34b/c*	0.915 (0.833–0.997)	13.0	0.870 (0.664–0.972)	0.875 (0.676–0.973)	46.7 (8.4–258.9)
			17.8	0.565 (0.345–0.768)	0.958 (0.789–0.999)	29.9 (3.4–260.6)
			21.0	0.348 (0.164–0.573)	1.000 (0.858–1.000)	N/A
	SFRP1	0.752 (0.615–0.889)	45.0	0.348 (0.164–0.573)	0.875 (0.676–0.973)	3.7 (0.8–16.4)
≥25mm	*miR34b/c*	0.778 (0.000–1.000)	15.0	0.667 (0.410–0.867)	0.667 (0.094–0.991)	4.0 (0.3–53.5)
<25mm	*SFRP1*	0.695 (0.450–0.941)	51.0	0.200 (0.005–0.716)	1.000 (0.839–1.000)	N/A

DOI:10.1158/1940-6207.CAPR-10-0214

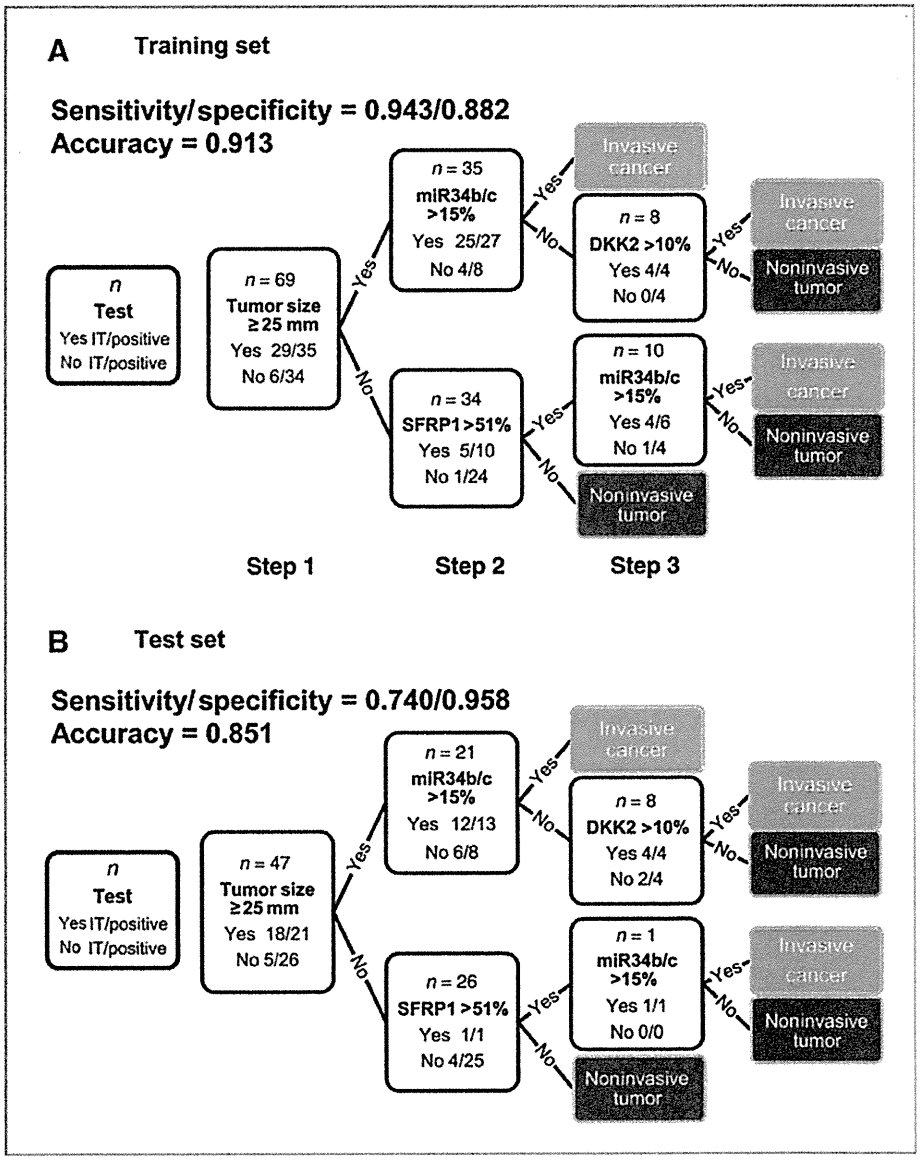

Figure 4. A diagnostic tree to classify invasive and noninvasive tumors on the basis of methylation levels detected in wash fluid. A, a diagnostic tree constructed on the basis of the training set. The majority class in each leaf is the predictive class. B, the application of the diagnostic tree to the test set.

noninvasive tumors. It is generally accepted that colonic epithelial cells are exfoliated into the lumen, that cancer cells can be detected among stool-derived exfoliated cells, and that stool DNA/RNA derived from exfoliated cells may be useful for diagnosis (36, 37). In that context, there are several possible explanations for the higher concentration of DNA from invasive tumor cells in colonoscopy wash fluid. Resistance to apoptosis and loss of cell adhesion are characteristic features of invasive cells (38, 39), which may facilitate the survival of exfoliated cells allowing for good DNA quality. Although we did not detect high levels of methylation in wash fluid from noninvasive tumors, we did obtain relatively large amounts of DNA. The origin of the DNA remains to be determined, but it may be derived from both tumor cells and normal cells such as white blood cells.

Our findings suggest that the high levels of *mir-34b/c* methylation in invasive tumors could be applied to predict invasiveness by using stool DNA. To date, most diagnostic methods for detecting colorectal tumors based on DNA methylation utilize qualitative methylation analysis (16, 19, 20). Using sensitive and quantitative analysis such as BEAMing technology (18), it should be possible to predict the invasiveness of tumors by using stool DNA. Further study to optimize the threshold will be necessary, however.

In summary, high levels of DNA methylation in colorectal washing fluid were correlated with invasiveness of colorectal lesions. Combining endoscopic and DNA

DOI:10.1158/1940-6207.CAPR-10-0214

methylation analyses may facilitate accurate preoperative staging of colorectal cancer.

Disclosure of Potential Conflicts of Interest

No potential conflicts of interest were disclosed.

Acknowledgments

The authors thank Dr. William F. Goldman for editing the manuscript.

Grant Support

This study was supported in part by Grants-in-Aid for Scientific Research on Priority Areas (T. Tokino, K. Imai, and M. Toyota), Grants-in-Aid for Scientific Research (S) from the Japan Society for Promotion of Science (K. Imai), a Grant-in-Aid for the Third-term Comprehensive 10-year Strategy for Cancer Control (M. Toyota), and a Grant-in-Aid for Cancer Research from the Ministry of Health, Labor, and Welfare, Japan (M. Toyota).

The costs of publication of this article were defrayed in part by the payment of page charges. This article must therefore be hereby marked *advertisement* in accordance with 18 U.S.C. Section 1734 solely to indicate this fact.

Received August 25, 2010; revised January 19, 2011; accepted January 27, 2011; published online May 4, 2011.

References

1. Jemal A, Siegel R, Ward E, Hao Y, Xu J, Murray T, et al. Cancer statistics, 2008. CA Cancer J Clin 2008;58:71–96.
2. Davies RJ, Miller R, Coleman N. Colorectal cancer screening: prospects for molecular stool analysis. Nat Rev Cancer 2005;5:199–209.
3. Osborn NK, Ahlquist DA. Stool screening for colorectal cancer: molecular approaches. Gastroenterology 2005;128:192–206.
4. Kwok H, Bissett IP, Hill GL. Preoperative staging of rectal cancer. Int J Colorectal Dis 2000;15:9–20.
5. Yamada I, Okabe S, Enomoto M, Sugihara K, Yoshino N, Tetsumura A, et al. Colorectal carcinoma: in vitro evaluation with high-spatial-resolution 3D constructive interference in steady-state MR imaging. Radiology 2008;246:444–53.
6. Hurlstone DP, Cross SS, Adam I, Shorthouse AJ, Brown S, Sanders DS, et al. A prospective clinicopathological and endoscopic evaluation of flat and depressed colorectal lesions in the United Kingdom. Am J Gastroenterol 2003;98:2543–9.
7. Kudo S, Kashida H, Tamura T, Kogure E, Imai Y, Yamano H, et al. Colonoscopic diagnosis and management of nonpolypoid early colorectal cancer. World J Surg 2000;24:1081–90.
8. Soetikno R, Friedland S, Kaltenbach T, Chayama K, Tanaka S. Nonpolypoid (flat and depressed) colorectal neoplasms. Gastroenterology 2006;130:566–76; quiz 88–9.
9. Bianco MA, Rotondano G, Marmo R, Garofano ML, Piscopo R, de Gregorio A, et al. Predictive value of magnification chromoendoscopy for diagnosing invasive neoplasia in nonpolypoid colorectal lesions and stratifying patients for endoscopic resection or surgery. Endoscopy 2006;38:470–6.
10. Matsuda T, Fujii T, Saito Y, Nakajima T, Uraoka T, Kobayashi N, et al. Efficacy of the invasive/non-invasive pattern by magnifying chromoendoscopy to estimate the depth of invasion of early colorectal neoplasms. Am J Gastroenterol 2008;103:2700–6.
11. Kanao H, Tanaka S, Oka S, Hirata M, Yoshida S, Chayama K. Narrow-band imaging magnification predicts the histology and invasion depth of colorectal tumors. Gastrointest Endosc 2009;69:631–6.
12. Markowitz SD, Bertagnolli MM. Molecular origins of cancer: Molecular basis of colorectal cancer. N Engl J Med 2009;361:2449–60.
13. Wong JJ, Hawkins NJ, Ward RL. Colorectal cancer: a model for epigenetic tumorigenesis. Gut 2007;56:140–8.
14. Issa JP. CpG island methylator phenotype in cancer. Nat Rev Cancer 2004;4:988–93.
15. Jones PA, Baylin SB. The epigenomics of cancer. Cell 2007;128:683–92.
16. Glöckner SC, Dhir M, Yi JM, McGarvey KE, Van Neste L, Louwagie J, et al. Methylation of TFPI2 in stool DNA: a potential novel biomarker for the detection of colorectal cancer. Cancer Res 2009;69:4691–9.
17. Hellebrekers DM, Lentjes MH, van den Bosch SM, Melotte V, Wouters KA, Daenen KL, et al. GATA4 and GATA5 are potential tumor suppressors and biomarkers in colorectal cancer. Clin Cancer Res 2009;15:3990–7.
18. Li M, Chen WD, Papadopoulos N, Goodman SN, Bjerregaard NC, Laurberg S, et al. Sensitive digital quantification of DNA methylation in clinical samples. Nat Biotechnol 2009;27:858–63.
19. Müller HM, Oberwalder M, Fiegl H, Morandell M, Goebel G, Zitt M, et al. Methylation changes in faecal DNA: a marker for colorectal cancer screening? Lancet 2004;363:1283–5.
20. Zou HZ, Yu BM, Wang ZW, Sun JY, Cang H, Gao F, et al. Detection of aberrant p16 methylation in the serum of colorectal cancer patients. Clin Cancer Res 2002;8:188–91.
21. Ahuja N, Li Q, Mohan AL, Baylin SB, Issa JP. Aging and DNA methylation in colorectal mucosa and cancer. Cancer Res 1998;58:5489–94.
22. Issa JP, Ottaviano YL, Celano P, Hamilton SR, Davidson NE, Baylin SB. Methylation of the oestrogen receptor CpG island links ageing and neoplasia in human colon. Nat Genet 1994;7:536–40.
23. Park SJ, Rashid A, Lee JH, Kim SG, Hamilton SR, Wu TT. Frequent CpG island methylation in serrated adenomas of the colorectum. Am J Pathol 2003;162:815–22.
24. Satoh A, Toyota M, Itoh F, Sasaki Y, Suzuki H, Ogi K, et al. Epigenetic inactivation of CHFR and sensitivity to microtubule inhibitors in gastric cancer. Cancer Res 2003;63:8606–13.
25. Toyota M, Suzuki H, Sasaki Y, Maruyama R, Imai K, Shinomura Y, et al. Epigenetic silencing of microRNA-34b/c and B-cell translocation gene 4 is associated with CpG island methylation in colorectal cancer. Cancer Res 2008;68:4123–32.
26. Kusano M, Toyota M, Suzuki H, Akino K, Aoki F, Fujita M, et al. Genetic, epigenetic, and clinicopathologic features of gastric carcinomas with the CpG island methylator phenotype and an association with Epstein-Barr virus. Cancer 2006;106:1467–79.
27. Sato H, Suzuki H, Toyota M, Nojima M, Maruyama R, Sasaki S, et al. Frequent epigenetic inactivation of DICKKOPF family genes in human gastrointestinal tumors. Carcinogenesis 2007;28:2459–66.
28. Suzuki H, Watkins DN, Jair KW, Schuebel KE, Markowitz SD, Chen WD, et al. Epigenetic inactivation of SFRP genes allows constitutive WNT signaling in colorectal cancer. Nat Genet 2004;36:417–22.
29. Tanaka S, Kaltenbach T, Chayama K, Soetikno R. High-magnification colonoscopy (with videos). Gastrointest Endosc 2006;64:604–13.
30. Winawer SJ, Zauber AG, Fletcher RH, Stillman JS, O'Brien MJ, Levin B, et al. Guidelines for colonoscopy surveillance after polypectomy: a consensus update by the US Multi-Society Task Force on Colorectal Cancer and the American Cancer Society. Gastroenterology 2006;130:1872–85.
31. Matsubayashi H, Canto M, Sato N, Klein A, Abe T, Yamashita K, et al. DNA methylation alterations in the pancreatic juice of patients with suspected pancreatic disease. Cancer Res 2006;66:1208–17.
32. Pattani KM, Zhang Z, Demokan S, Glazer C, Loyo M, Goodman S, et al. Endothelin receptor type B gene promoter hypermethylation in salivary rinses is independently associated with risk of oral cavity cancer and premalignancy. Cancer Prev Res 2010;3:1093–103.
33. Watanabe Y, Kim HS, Castoro RJ, Chung W, Estecio MR, Kondo K, et al. Sensitive and specific detection of early gastric cancer with DNA methylation analysis of gastric washes. Gastroenterology 2009;136:2149–58.

DOI:10.1158/1940-6207.CAPR-10-0214

34. Shen L, Toyota M, Kondo Y, Lin E, Zhang L, Guo Y, et al. Integrated genetic and epigenetic analysis identifies three different subclasses of colon cancer. Proc Natl Acad Sci U S A 2007;104:18654–9.
35. He L, He X, Lim LP, de Stanchina E, Xuan Z, Liang Y, et al. A microRNA component of the p53 tumour suppressor network. Nature 2007; 447:1130–4.
36. White V, Scarpini C, Barbosa-Morais NL, Ikelle E, Carter S, Laskey RA, et al. Isolation of stool-derived mucus provides a high yield of colonocytes suitable for early detection of colorectal carcinoma. Cancer Epidemiol Biomarkers Prev 2009;18:2006–13.
37. Zhao C, Ivanov I, Dougherty ER, Hartman TJ, Lanza E, Bobe G, et al. Noninvasive detection of candidate molecular biomarkers in subjects with a history of insulin resistance and colorectal adenomas. Cancer Prev Res 2009;2:590–7.
38. Brown JM, Attardi LD. The role of apoptosis in cancer development and treatment response. Nat Rev Cancer 2005;5: 231–7.
39. Christofori G. Changing neighbours, changing behaviour: cell adhesion molecule-mediated signalling during tumour progression. EMBO J 2003;22:2318–23.

Interferon-α/β and Anti-Fibroblast Growth Factor Receptor 1 Monoclonal Antibody Suppress Hepatic Cancer Cells In Vitro and In Vivo

Shigeru Sasaki[1]*, Tadao Ishida[1], Minoru Toyota[2]*, Akinobu Ota[3], Hiromu Suzuki[1,2], Akinori Takaoka[4], Hiroshi Yasui[1,2], Hiroyuki Yamamoto[1], Hideyasu Takagi[1], Masahiro Maeda[3], Tsutomu Seito[3], Masayuki Tsujisaki[5], Yasuhisa Shinomura[1], Kohzoh Imai[6]

1 First Department of Internal Medicine, Sapporo Medical University, Sapporo, Japan, 2 Department of Molecular Biology, Sapporo Medical University, Sapporo, Japan, 3 Immuno-Biological Laboratories Co., Ltd., Fujioka, Japan, 4 Division of Signaling in Cancer and Immunology, Institute for Genetic Medicine, Hokkaido University, Sapporo, Japan, 5 Department of Gastroenterology and Hematology, Tenshi Hospital, Sapporo, Japan, 6 Division of Novel Therapy for Cancer, The Advanced Clinical Research Center, The Institute of Medical Science, The University of Tokyo, Tokyo, Japan

Abstract

Background: Hepatocellular carcinoma (HCC) is the most commonly occurring primary liver cancer and ranks as the fifth most frequently occurring cancer, overall, and the third leading cause of cancer deaths, worldwide. At present, effective therapeutic options available for HCC are limited; consequently, the prognosis for these patients is poor. Our aim in the present study was to identify a novel target for antibody therapy against HCC.

Methodology/Principal Findings: We used Western blot and flow cytometric and immunocytochemical analyses to investigate the regulation of FGFR1 expression by interferon-α/β in several human hepatic cancer cell lines. In addition, we tested the efficacy of combined treatment with anti-FGFR1 monoclonal antibody and interferon-α/β in a murine xenograft model of human HCC. We found that interferon-α/β induces expression of FGFR1 in human HCC cell lines, and that an anti-FGFR1 monoclonal antibody (mAb) targeting of the induced FGFR1 can effectively inhibit growth and survival of HCC cells *in vitro* and *in vivo*. Moreover, the combination of interferon-α, anti-FGFR1 mAb and peripheral blood mononuclear cells (PBMCs) exerted a significant antitumor effect *in vitro*.

Conclusions: Our results suggest that the combined use of an anti-FGFR1 antibody and interferon-α/β is a promising approach to the treatment of HCC.

Citation: Sasaki S, Ishida T, Toyota M, Ota A, Suzuki H, et al. (2011) Interferon-α/β and Anti-Fibroblast Growth Factor Receptor 1 Monoclonal Antibody Suppress Hepatic Cancer Cells In Vitro and In Vivo. PLoS ONE 6(5): e19618. doi:10.1371/journal.pone.0019618

Editor: Young Nyun Park, Yonsei University College of Medicine, Republic of Korea

Received October 9, 2010; **Accepted** April 11, 2011; **Published** May 9, 2011

Funding: This study was supported in part by Grants-in-Aid for Scientific Research on Priority Areas from the Ministry of Education, Culture, Sports, Science, and Technology (17016060 to KI and TI); Grants-in-Aid for Scientific Research (C) from the Japan Society for Promotion of Science (21590853 to SS); Grant-in-Aid for Exploratory Research from the Japan Society for Promotion of Science (17659218 to SS and KI). The funders had no role in study design, data collection and analysis, decision to publish, or preparation of the manuscript.

Competing Interests: A. Ota, M. Maeda, T. Seito are employees of Immuno-Biological Laboratories Co., Ltd. This does not alter the authors' adherence to all the PLoS ONE policies on sharing data and materials with other investigators.

* E-mail: ssasaki@sapmed.ac.jp (SS); mtoyota@sapmed.ac.jp (MT)

Introduction

Hepatocellular carcinoma (HCC) is the most commonly occurring primary liver cancer and ranks as the fifth most frequently occurring cancer, overall, and the third leading cause of cancer deaths, worldwide [1]. At present, surgery, percutaneous therapies such as ethanol injection and radiofrequency ablation, and transcatheter therapies such as arterial chemoembolization are employed in the treatment of HCC. These approaches can selectively remove and kill cancer cells, which makes them useful for control of the local tumor; however, they are not sufficient to improve the prognosis of HCC patients, as the disease readily recurs due to blood-born metastases (e.g., intrahepatic metastasis and vascular infiltration) or the development of new HCCs (multicentric carcinogenesis). Consequently, the 1-year and 3-year survival rates for HCC are only 36% and 17%, respectively [2]. The weaknesses of the current HCC treatments include incomplete inhibition of multicentric carcinogenesis, difficulties in controlling intraportal infiltration, and the inability to prevent deterioration of hepatic functional reserve or foster its restoration. Thus development of new treatments that improve the prognosis of HCC patients and which can also be used in elderly and advanced stage patients would be highly desirable.

Targeting cell surface molecules using mAbs is an emerging strategy in cancer therapy, and mAbs against cancer-related surface molecules such as EGFR, HER2 and CD20 have been successfully employed [3,4,5]. However, cell surface expression of antigenic molecules is often weak and heterogeneous, which prevents the efficient targeting of tumors [6] and, to date, only a few pilot studies examining expression of HCC-associated antigens have been carried out [7].

Interferons (IFNs), which are widely used for the treatment of neoplasias and viral diseases, enhance expression of several cell surface molecules both *in vitro* and in xenograft tumor models [8,9]. Induction of gene expression by IFN is a complex phenomenon that involves activation of target genes via phosphorylation of STATs by JAK kinase [10]. In addition, IFNs can induce expression of interferon regulatory factors (IRFs) and transcription factors, which then induce genes involved in apoptosis and immune responses [11]. IFNs are already being used to treat most hepatitis patients, and their effects suggest targeting cell surface molecules induced by IFN may be a useful strategy for treating HCC. Our aim in the present study was to use HCC cell lines and a murine xenograft model of human HCC to examine the changes in gene expression induced by IFN and to identify potential targets for antibody therapy. Our findings suggest IFN-α/β-induced fibroblast growth factor receptor 1 (FGFR1) could be a novel therapeutic target for the treatment of HCC.

Results

Induction of FGFR1 expression by IFN-α/β in HCC xenografts

To identify genes up-regulated by IFN in HCC cells, we performed a microarray analysis using cDNA prepared from tumors grown in SCID mice subcutaneously administrated HepG2 cells, a human hepatic cancer cell line. The results of the microarray analysis are summarized in Figure 1A. Among the genes up-regulated by IFN was *FGFR1*, which encodes a receptor tyrosine kinase. Real-time PCR analysis confirmed induction of *FGFR1* transcription by both IFN-α and IFN-β (Figure S1), and corresponding increases in FGFR1 protein were observed in HepG2, Huh-7 and CHC4 cells (Figure 1B–D). We then used immunohistochemical staining to examine the distribution of IFN-α/β-induced FGFR1 within the tumors and found that levels of FGFR1 were increased at the cell membrane and in the cytoplasm of HCC cells (Figure 1E).

Development of an anti-FGFR1 monoclonal antibody

We developed novel anti-FGFR1 mAbs by immunizing BALB/c mice with an FGFR1 expression vector. Six antibodies recognizing FGFR1 were isolated from the mice, two of which, designated A2C9-1 and A2D11-1, showed strong affinity in ELISAs and were characterized further. For kinetic analyses, the extracellular domain of FGFR1 was covalently coupled to a CM-5 sensor chip at low density (215 response units of FGFR1), after which we determined the Kd values for A2C9-1 and A2D11-1 to be 209 nM and 7.03 μM, respectively (Figure S2A). Thus A2C9-1 showed the strongest affinity for FGFR1. Flow cytometric analysis confirmed that A2C9-1 reacts with FGFR1 (Figure 2), and Western blot analysis showed the molecular weight of the ectopically expressed FGFR1 to be around 115 kDa (Figure S2B).

Anti-FGFR1 mAbs inhibit HCC cell growth in vitro

We next examined the effects of A2C9-1 and A2D11-1 mAbs on the growth of hepatic cancer cells (Figure 3). IFN-α showed some antitumor activity against hepatic cancer cells, and weak growth suppression was seen when A2C9-1 or A2D11-1 was added to cultures in the absence of IFN-α. On the other hand, treatment with a combination of A2C9-1 and IFN-α significantly reduced cell survival, as compared to treatment with IFN-α alone ($P = 0.01$) (Figure 3). The effect of A2D11-1 in combination with IFN-α was no greater than the effect of IFN-α alone.

Effects of A2C9-1 with and without IFN-α in a mouse xenograft tumor model

We next tested the antitumor effects of an anti-FGFR1 mAb in a mouse xenograft model of human HCC (Figure 4A and B). In mice treated with only A2C9-1 or IFN-α, tumor volumes did not differ from the control group administered PBS. However, treatment with IFN-α+A2C9-1 had an inhibitory effect on tumor growth, though the suppression was not statistically significant. Finally, in mice treated with IFN-α+A2C9-1+PBMCs (peripheral blood mononuclear cells), there was a significant antitumor effect, as compared to groups treated with PBS ($p = 0.026$), INF-α ($p = 0.03$), A2C9-1 ($p = 0.014$), PBMC ($p = 0.022$) or IFN-α+PBMCs ($p = 0.007$). In fact, the tumor disappeared in 2 of the 4 animals tested. During the course of the experiments we detected no cytotoxicity against normal hepatocytes (data not shown). Histological analysis revealed marked infiltration by mononuclear cells of the residual tumor tissues from mice treated with IFN-α+A2C9-1+PBMCs, but no such infiltration was observed in tumor tissues from mice in the other groups (Figure S3).

IFN enhances accumulation of anti-FGFR1 mAb within tumors

To further confirm that the observed regression of the xenografts was related to the treatment with A2C9-1 mAb, Alexa Fluor 680-conjugated A2C9-1 was injected into the tail veins of tumor-bearing SCID mice, after which the targeting of the tumor by A2C9-1 was evaluated in the same animals at different time points using an optical molecular imaging system (Figure 5A and B). In mice pretreated with IFN-α, A2C9-1 selectively and time-dependently accumulated within the tumors during the period from 24 h to 192 h after its administration. By contrast, only negligible levels of mAb were detected in control mice administered A2C9-1+PBS. We also confirmed that there was no accumulation of an Alexa Fluor 680-conjugated control antibody (data not shown). It thus appears that IFN-α enhances the accumulation of anti-FGFR1 mAb *in vivo*, most likely by up-regulating FGFR1.

Discussion

In this study, we found that FGFR1 can serve as a novel target for antibody therapy in HCC. More specifically, combined treatment with IFN-α/β and an anti-FGFR1 mAb (A2C9-1) showed strong growth suppressive effects on human HCC cells *in vitro* and *in vivo*. Five isoforms of the transmembrane receptor FGFR (FGFR1–4 and FGFR5/1L) are known to be expressed in mammals [12]. Each consists of three extracellular immunoglobulin-like domains, a transmembrane domain, and two intracellular tyrosine kinase domains. FGF binds to the FGFR via two of the immunoglobulin-like domains (II and III). During FGFR expression, alternative splicing of *FGFR* transcripts produces multiple splice variants with different tissue-specific ligand specificities [13]. Among them, FGFR1 has been shown to be expressed in HCC and is known to promote the development of HCC in response to carcinogenic stimulation [14]. FGFR1 is not expressed in noncancerous hepatocytes. FGFR1-mediated signaling is involved in cancer cell growth and infiltration, as well as in angiogenesis [15], which is already a target for antitumor therapies [16]. In addition, previous studies have shown elevated expression of FGFR ligands, including FGF1 and FGF2, in primary HCC tissues and hepatic cancer cell lines [17,18,19,20], strongly suggesting FGF signaling plays a key role in the development of HCC. These characteristics make FGFR1 an attractive molecular target for treating HCC.

A

Gene name	Fold change
Tie-2	82.3
hRAD50	43
TRT (hEST1, TERT)	29.2
ERα (Estrogen receptor α)	24.3
KKIALRE	20.7
FADD (MORT1)	19.6
JAK3	16.6
β-D glucuronidase	16.1
PDGFα	14.5
IL-2Rβ (F2 R2)	13.4
Integrinαllb (CD41)	11.6
Cytidine deaminase	11.1
APC	10.8
Cdc27 (nuc2 homolog)	10.2
MUC-2 (Mucin 2)	9.8
L-Selectin	9.8
FGFR-1 (Flg)	9.4
Flt-1	9.4
Ral B	8.9
hdlg-1 (dlg1)	8.6
Integrinα8	8.6
VHL (von Hippel-Lindau syndrome)	8.3
PMS1	8.2
cyclin T	8
Notch1 (TAN1)	7.2
Notch3	7
Laminin β-2	6.9
Midkine	6.8
Ras-GAP	6.6
TC 21	6.5
Bik (NBK)	5.3

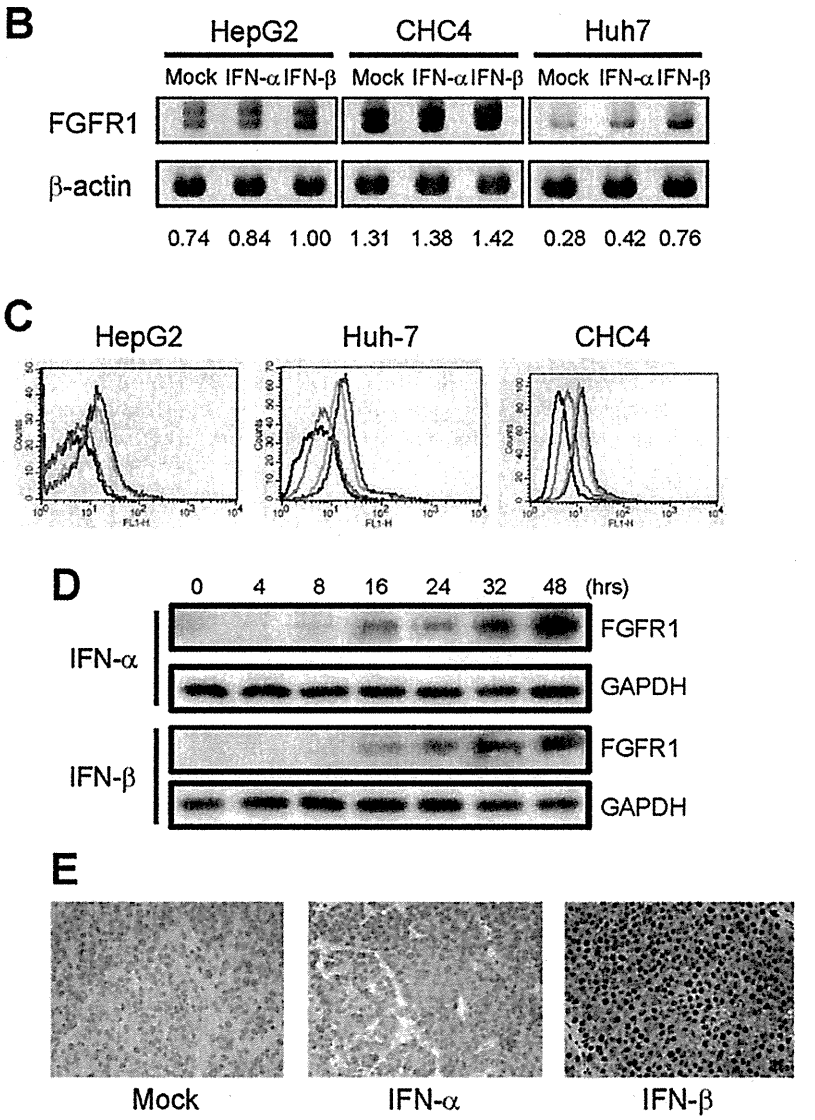

Figure 1. Induction of FGFR1 by IFN-α/β treatment in hepatic cancer cells. A, Summary of genes induced by IFN-α in hepatic cancer cell lines and HepG2-xenografts. Expression of genes induced by IFN-α was examined using DNA array analysis, and expression of *FGFR1* was found to be strongly induced. B, Western blot showing IFN-α/β-induced expression of FGFR1 in human hepatic cancer cells. Relative protein levels are indicated below. C, Flow cytometric analysis showing IFN-α/β-induced expression of FGFR1 in human hepatic cancer cells: black, no antibody; green, no IFN; Pink, IFN-α; Blue, IFN-β. D, Western blot showing the time course of FGFR1 expression after treatment with IFN-α/β. The immunoblots were done using total lysates from HepG2-xenografts. E, IFN-α/β-induced FGFR1 expression in excised tissues from HepG2-xenografts. FGFR1 was stained using anti-FGFR1 antibody.
doi:10.1371/journal.pone.0019618.g001

One major problem with antibody therapy against cancer is the weak and heterogeneous expression of cell surface antigens. To overcome this problem, we examined genes up-regulated by IFN in HCC xenografts. We found that expression of FGFR1 is induced by IFN-α/β and that treating HCC cells with a combination of IFN-α/β and an anti-FGFR1 mAb effectively inhibits the growth and survival of HCC cells. Thus, one reason for the insufficient therapeutic effect of anticancer drugs targeting FGFR1 appears to be is that, without induction, expression of FGFR1 on cancer cells is not sufficient for effective treatment. Consistent with this idea, our immunohistochemical analysis showed expression of FGFR1 to be very low in untreated HCC cells. Notably, epidermal growth factor receptor (EGFR) is also up-regulated by IFN [21], and this up-regulation of EGFR is a crucial factor underlying the susceptibility of affected cancer cells to anti-EGFR antibody therapy [22]. Taken together, these findings suggest treatment with a combination of IFN and an antibody may be an effective therapeutic strategy against various types of cancer.

The molecular mechanism by which IFN-α/β induces FGFR1 expression remains unknown. It is known, however, that the antitumor and antiviral effects of IFN involve changes in the transcriptional regulation of various genes [23], and that IFN-inducible genes contain an interferon response element (ISRE) in

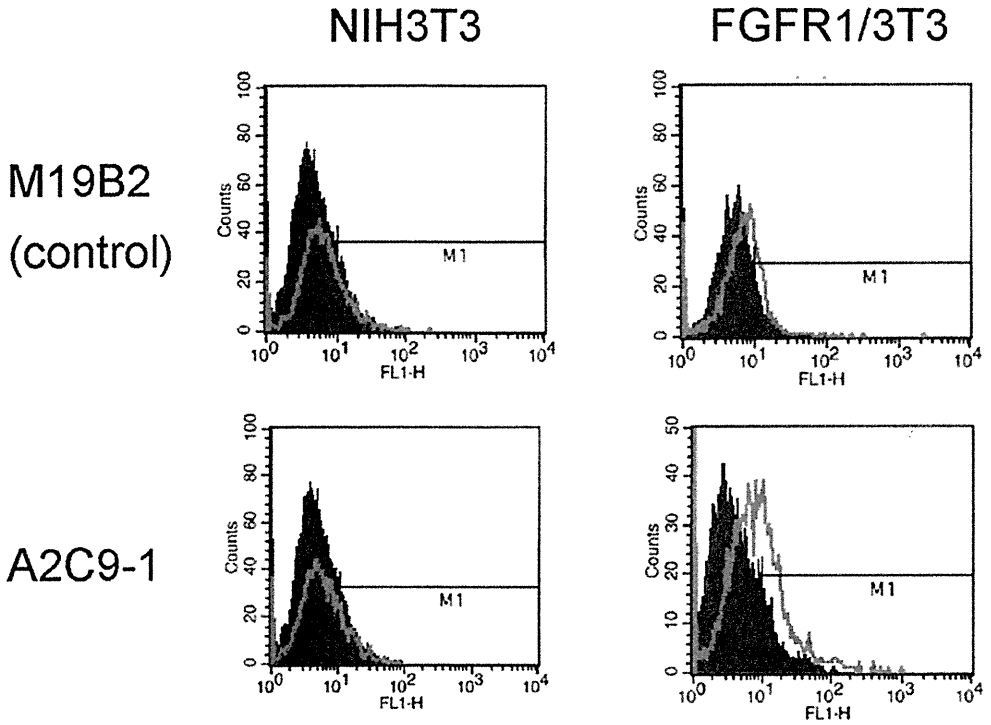

Figure 2. Development of anti-FGFR1 mAbs. Flow cytometric analysis showing the expression level of FGFR1 and specificity of A2C9-1 mAb. Left: the graphs show the results obtained with lysates from NIH3T3 cells into which M19B2 cDNA introduced (control). Right: the graphs show the results with lysates from NIH3T3 cells into which full-length FGFR1 cDNA was introduced.
doi:10.1371/journal.pone.0019618.g002

their promoter regions [24]. By using a transcription factor search program, we identified several putative ISREs in the 5′ UTR of FGFR1, suggesting that FGFR1 could be a direct target of type I IFN (data not shown). Further study will be necessary to determine precisely how interferon induces FGFR1.

We also do not yet fully understand the molecular mechanism by which our antibody exerted its anti-tumor effect, though there are several possibilities. Many of the tumor-expressed targets of therapeutic antibodies are growth factor receptors. For example, anti-EGFR antibodies, including Cetuximab, have been shown to block growth factor signaling by preventing the ligand from binding to its receptor, or by preventing receptor dimerization [25]. It is highly likely that A2C9-1 suppresses tumor cell growth through a similar mechanism by targeting IFN-induced FGFR1. It was also reported that the binding of an antibody to a growth factor receptor results in the internalization of the antibody-receptor complex, and the down-regulation of downstream signaling [26]; however, we observed no A2C9-1-induced internalization in cancer cells (data not shown). Thirdly, antibodies against growth factor receptors also exert growth suppressing effects via the immune system [27]. Here, for example, we showed that IFN-α/β enhances the surface expression of FGFR1, perhaps enabling an anticancer effect based on antibody-dependent cell-mediated cytotoxicity to accompany the binding of anti-FGFR1 mAb to the receptor. The results of our *in vivo* experiment showing the importance of PBMCs to the antitumor effects of A2C9-1 is consistent with the idea that this antibody strongly stimulates antibody-dependent cell-mediated cytotoxicity.

In summary, we found that IFN-α/β induces expression of FGFR1 and that treatment with a combination of IFN-α/β and an anti-FGFR1 mAb suppresses HCC cell growth *in vitro* and *in vivo*. We also confirmed that IFN-α/β enhances the accumulation of the anti-FGFR1 mAb within tumors. This treatment protocol selectively inhibits the growth of HCC cells without affecting normal cells, which suggests it could be used in the treatment of HCC without reducing hepatic preliminary performance. We therefore suggest that our results may provide the basis for a novel approach to the treatment of HCC, for which there is no effective therapy at the moment.

Materials and Methods

Cell lines and experimental animals

Human hepatic cancer cell lines (HepG2, Huh-7 and CHC4) were obtained from the Japanese Collection of Research Bioresources (Tokyo, Japan) and cultured as recommended. Cells were maintained in Dulbecco's modified Eagle's medium supplemented with 10% fetal bovine serum and penicillin/streptomycin at 37°C under an atmosphere of humidified air with 5% CO_2. Peripheral blood mononuclear cells (PBMCs) were isolated from healthy volunteers using Ficoll-Paque (GE Healthcare Life Science, Uppsala, Sweden) and used as effector cells in SCID mice. All donors provided written informed consent before collection in accordance with the Declaration of Helsinki, and all protocols using human samples were approved by the institutional review board of Sapporo Medical University. Whole PBMCs (1×10^7) suspended in 0.2 ml of RPMI 1640 were intraperitoneally injected into each SCID mouse. All animal experiments were conducted in accordance with accepted standards of animal care and approved by the Institutional Animal Care and Use Committee of Sapporo Medical University.

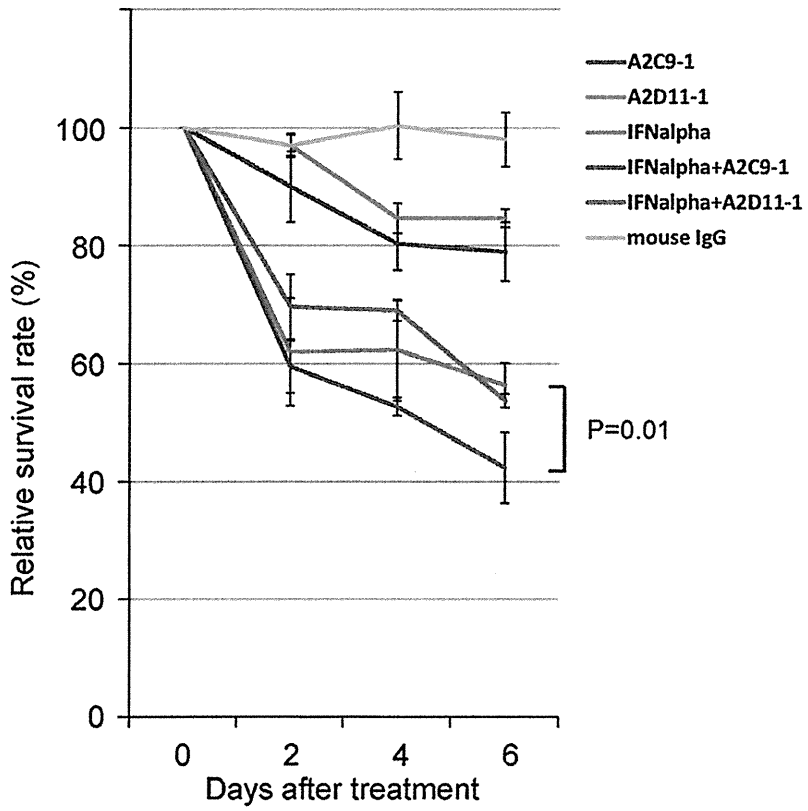

Figure 3. Antitumor activity of anti-FGFR1 mAbs in combination with IFN-α *in vitro*. In the graph, the survival rate among cultured HepG2 HCC cells is shown on the vertical axis, and the incubation time after administration of the indicated drugs is shown on the horizontal axis. PBS is the negative control. Symbols and bars represent means ± SD. Note that treatment with a combination of A2C9-1 and IFN-α significantly reduced cell survival, as compared to treatment with IFN-α alone ($P = 0.01$).
doi:10.1371/journal.pone.0019618.g003

Microarray analysis

For microarray analysis, HepG2 cells (1×10^6 cells) were initially xenografted into severe combined immunodeficient (SCID) mice. Three weeks later, when the resultant tumor had reached 6–7 mm in diameter, IFN-α (OIF®; Otsuka Pharmaceutical Co., Ltd., Tokushima, Japan) was subcutaneously injected at a dose of 2000 U/mouse. Samples of tumor tissue were collected before and 24 h after injection of the IFN-α. RNA was extracted from the collected tissues using Trizol (Invitrogen, Carlsbad, CA, USA) and reverse transcribed to cDNA using Superscript III (Invitrogen). The cDNA was then reacted using Gene Navigator cDNA Array Filter-human cancer (Toyobo, Osaka, Japan) and subjected to DNA array analysis using a Fluor-S Multi Imager (Bio-Rad Laboratories, Hercules, CA, USA).

Real-time RT-PCR analysis

HepG2 (1×10^6 cells) cells were subcutaneously xenografted into the backs of SCID mice. When the inoculated tumor reached 10 mm in diameter, IFN-α (OIF®) or IFN-β (Feron®; manufactured by Toray Industries, Inc., Tokyo, Japan) was administered intravenously at a dose of 2000 U/mouse, and samples of tumor tissue were collected 0, 1, 3, 8, 24 and 48 h after administration. Total RNA was purified from the samples using a RNeasy Kit (QIAGEN, Hilden, Germany), and single-strand cDNA was synthesized from 1 μg of total RNA using a First-Strand cDNA Synthesis Kit (GE Healthcare Life Science, Uppsala, Sweden). Real-time quantitative analysis was performed using SYBR Green I (Roche, Basel, Switzerland) with a LightCycler Real-time PCR system (Roche). Levels of FGFR1 and OAS1 (control) mRNA expression were normalized to the expression of GAPDH mRNA. Primer sets for FGFR1 (sense, 5′-GGA CGA TGT GCA GAG CAT CAA CTG-3′; anti-sense, 5′-AAC TTC ACT GTC TTG GCA GCC GG-3′), OAS1 (sense, 5′-CAT CCG CCT AGT CAA GCA CTG-3′; anti-sense, 5′-CCA CCA CCC AAG TTT CCT GTA-3′) and GAPDH (sense, 5′-GAA GGT GAA GGT CGG AGT C-3′; anti-sense, 5′-GAA GAT GGT GAT GGG ATT-TC-3′) were synthesized at Greiner Bio-One (Tokyo, Japan).

Western blot analysis

HepG2, Huh-7 or CHC4 cells were incubated for 48 h in the presence of IFN-α or IFN-β (1,000 IU/ml), after which the cells were lysed in sample buffer (50 mM Tris-HCl, pH 6.8, 6% 2-mercaptoethanol, 2% SDS, 0.004% bromophenol blue, and 10% glycerol). Proteins in samples of lysate were separated by 7.5% polyacrylamide gel electrophoresis and then transferred onto a nitrocellulose membrane (Bio-Rad Laboratories). After blocking the membrane with 2% bovine serum albumin (BSA) in PBS for 1 h at room temperature, it was incubated with anti-human FGFR1 antibody (sc-121, Santa Cruz Biotechnology, Santa Cruz, CA, USA) for 1 h at room temperature. The blot was then developed with 0.005% H_2O_2-3, 3′-diaminobenzidine using an immunoperoxidase ABC kit (Vectastain ABC kit, Vector Labs, Burlingame, CA, USA).

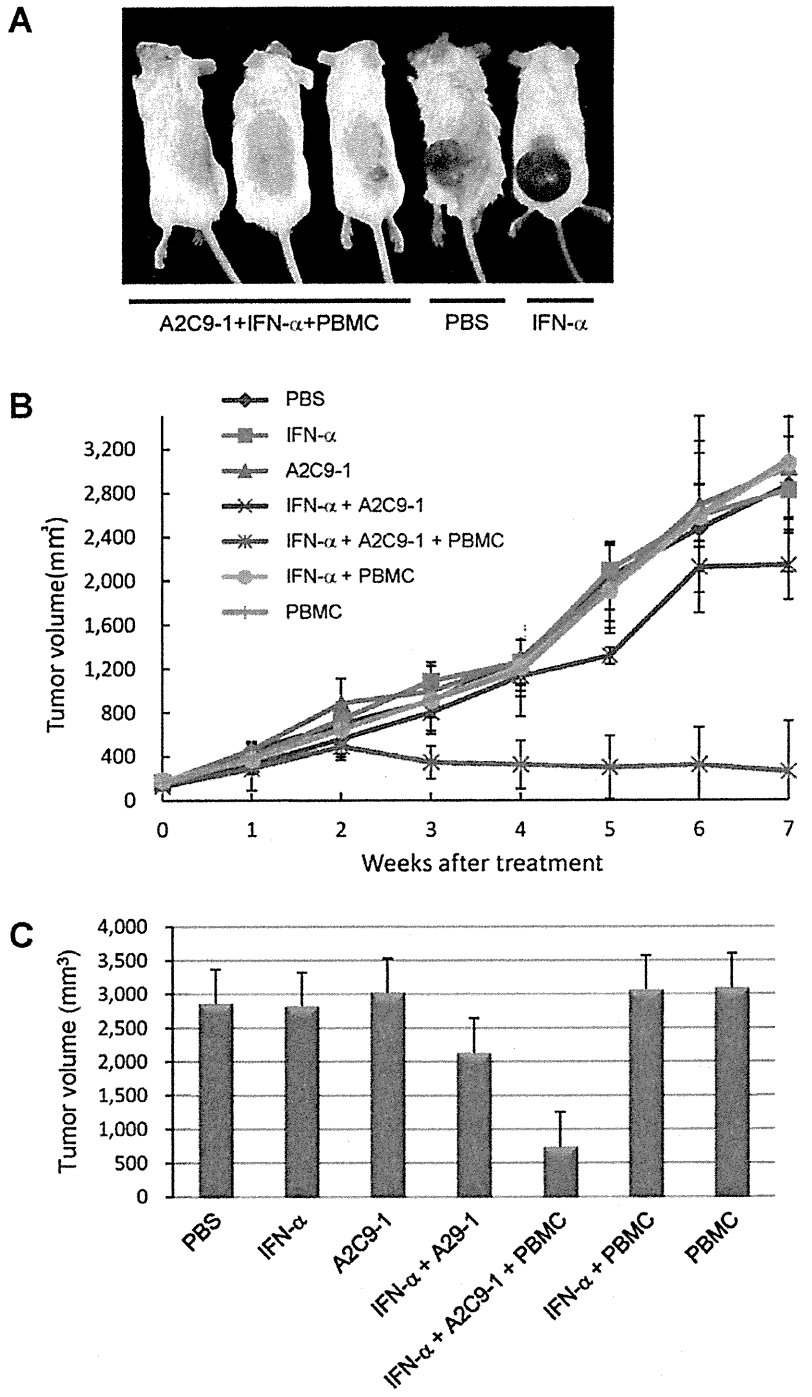

Figure 4. Antitumor activity of anti-FGFR1 mAb in combination with IFN-α in a murine xenograft tumor model of human HCC. A, Representative photos of tumor grafts on SCID mice. B, In the graph, the sizes of the tumors in each group (n = 4 mice per group) are shown on the vertical axis, and the elapsed time after treatment with the indicated drugs and cells is shown on the horizontal axis. Symbols and bars are means ± SD. C, Tumor volumes following treatment with the indicated drugs and cells. PBS is the negative control. Data are means ± SD.
doi:10.1371/journal.pone.0019618.g004

Flow cytometric analysis

Forty-eight hours after administration of IFN-α, expression of FGFR1 was assessed using flow cytometry. Cells in suspension (4×10^5 cells/tube) were washed with 2 mL of washing buffer (0.2% bovine serum albumin, 0.1% NaN_3/10 mmol/L phosphate-buffered saline, pH 7.4) and centrifuged at 300 *g* for 5 min at 4°C, after which the supernatant was removed. The remaining cell pellet was fixed in 0.25% paraformaldehyde for at least 15 min

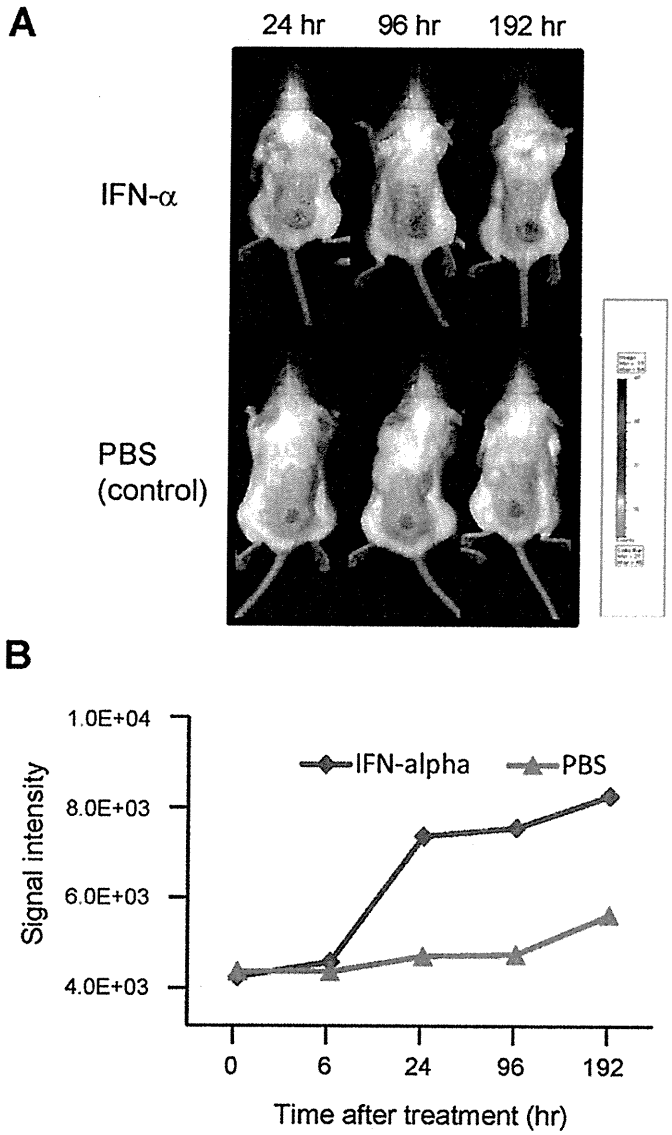

Figure 5. Accumulation of anti-FGFR1 mAb in tumor xenografts is enhanced by IFN-α. A, SCID mice were xenografted with 1×10^6 HepG2 cells, after which 50 μg of Cy5-conjugated A2C9-1 mAb was intravenously administrated via the tail vein. Mice were then imaged under anesthesia. B, Time course of the Cy5 signal intensity.
doi:10.1371/journal.pone.0019618.g005

in the dark at room temperature, washed twice with 2 mL washing buffer, incubated for 1 h in 70% methanol at 4°C, and then washed again. To examine expression of FGFR1, the fixed cells were incubated first with anti-FGFR1 antibody (1:100 dilution) for 1 h at 4°C. The cells were then washed twice and incubated for 30 min in 4 mL of fluorescein isothiocyanate-conjugated goat anti-mouse IgG on ice in the dark. After again washing the cells twice, they were suspended in 1 mL of washing buffer for analysis using a FACScan (Becton Dickinson Immunocytometry System, San Jose, CA, USA).

Analysis of FGFR1 expression in human hepatic cancer xenografts

HepG2 cells (1×10^6 cells) were xenografted into SCID mice. When the resultant tumor reached 10 mm in diameter, IFN-α (OIF®) or IFN-β (Feron®) was administered intraperitoneally or intravenously at a dose of 100 U/g, and 24 h later tumor tissues were collected. Western blot and immunohistochemical analyses were then performed using an anti-human FGFR1 antibody (sc-121; Santa Cruz Biotechnology).

Preparation of Anti-FGFR1 Antibody

A polynucleotide encoding the region extending from amino acid 1 to 822 of FGFR1 and represented by SEQ ID NO. 1 was amplified by PCR using full-length FGFR1 (Accession No. NM_000604) as a template with primers No. 5′-3 [(SEQ ID NO. 3): 5′-ACGGGATC-CAGGACCCTGGCTGGAGAGACA-3′] and No. 3′-3 [(SEQ ID NO. 4): 5′-AAGCTCGAGCCGCCGGAACCGCGGCCGGA-3′]. The amplified polynucleotide was inserted into pcDNA3.1

(Invitrogen, Carlsbad, CA, USA) to construct an expression vector that was administered as the immunizing antigen at a dose of 50 μg/mouse in a 50-μL volume at 1- or 2-week intervals. The antigen for the initial immunization was admixed with complete Freund's adjuvant, while the antigens for the second and subsequent administrations were admixed with incomplete Freund's adjuvant. Spleen monocytic cells from the immunized mouse and a fusion partner, X63-Ag8-653, were fused using polyethylene glycol-mediated cell fusion, which was followed by selection of a hybridoma using the method of Kinebuchi et al. [28]. Cells that had reacted with the immobilized FGFR1 were cultured in serum-free GIT medium (Wako Pure Chemical Industries, Ltd., Osaka, Japan) to produce mAbs until 80% of the cells had died. The cells were then removed from this medium by centrifugation (1,000 rpm, 15 min), and ammonium sulfate was added to 50% saturation and left overnight at 4°C. The resultant precipitates were recovered by centrifugation (1,000 rpm, 30 min) and dissolved in two-fold diluted binding buffer (Protein AMAPS II kit), after which the IgG was adsorbed onto a protein A column (GE Healthcare Life Science). After eluting the mAbs from the column, the eluate was dialyzed against PBS overnight to purify the antibodies, which yielded a number of mAbs recognizing FGFR1. One of those mAbs was designated A2C9-1 and was confirmed to recognize FGFR1 by Western blotting and FACS using samples of FGFR1 expressed in NIH3T3 cells.

Affinity measurement

The affinity of anti-FGFR1 mAbs for FGFR1 was determined based on surface plasmon resonance (SPR) using a Biacore 3000 device (Biacore AB, Uppsala, Sweden). The extracellular domain of FGFR1 was covalently coupled to a CM-5 sensor chip at low density (215 response units of FGFR1). Binding kinetics were then assessed using twofold serial dilutions of antibody at concentrations ranging from 500 to 0.08 nM in running buffer (PBS, pH 7.4, 0.005% (v/v), polysorbate 20 – filtered and degassed) at 25°C and a flow rate of 25 ml/min. The regeneration procedure consisted of three injections of 10 ml of 2.5 M guanidinium hydrochloride, after which the sensor chip was flushed for 5 min with running buffer. Statistics and data processing were performed using BIA evaluation software 4.0.1 and GraphPad Prism 4.02 (GraphPad Software Inc., San Diego, CA, USA). All SPR experiments were carried out at Biaffin GmbH & Co. KG (Kassel, Germany).

Assessing the effect of anti-FGFR1 mAb on hepatic cancer cell viability

To examine the effect of administering IFN-α (OIF®) in combination with anti-FGFR1 mAb (A2C9-1 or A2D11-1) to HCC cells, we assessed the survival rate of HepG2 cells in the presence and absence of IFN-α and/or anti-FGFR1 mAb. HepG2 cells were seeded into the wells of a 24-well plate to a density of 1×10^4 cells/well, after which anti-FGFR1 mAb, IFN-α or anti-FGFR1 mAb+IFN-α was added, and the culture was continued for 0 to 6 days. The cells were then detached using trypsin, and the survival rate was assessed using MTT assays. Antibody-free culture medium was added as negative control, and cells to which nothing was added were used as an additional control.

Therapeutic experiment with human hepatic cancer cells-xenografted mouse

HepG2 cells (5×10^6 cells/mouse) were xenografted subcutaneously into the backs of CB17-scid/scid mice. When the volumes of the tumors reached 100 mm^3, the mice were divided into 7 treatment groups: 1) Mice in the PBS group received intravenous injections of PBS (250 μL) and normal mouse IgG (100 μg). 2) The IFN-α group received intraperitoneal injections of IFN-α (OIF®: 2000 U) and normal mouse IgG (100 μg). 3) The antibody group received intravenous injections of PBS and anti-FGFR1 mAb (100 μg; A2C9-1). 4) The IFN-α+antibody group received intraperitoneal injections of IFN-α (2000 U) and intravenous injections of anti-FGFR1 mAb (100 μg). 5) The IFN-α+antibody+PBMC group received intraperitoneal injections of IFN-α (2000 U), intravenous injections of anti-FGFR1 mAb (100 μg) and intravenous administration of PBMCs (1×10^7 cells). 6) The IFN-α+PBMC group received intraperitoneal injections of IFN-α (2000 U) and intravenous administration of PBMCs (1×10^7 cells). 7) The PBMC group received intravenous administration of PBMCs (1×10^7 cells). Treatments were administered 5 times in total, beginning on day 0 and then 1 week later (w1), 2 weeks later (w2), 5 weeks later (w5) and 6 weeks later (w6). Only at w6, the antibody dose was increased to 200 μg/mouse. Each group contained 4 animals, and the size of tumor was measured as (major axis)×(minor axis)×2 weekly after initial administration. Tumors were harvested 1 week after the final treatment.

Immunophotodetection in tumor-bearing mice

HepG2 human HCC cells (1×10^6 cells) were xenografted into the backs of SCID mice. Three weeks later, when the inoculated tumor had reached about 10 mm in diameter, IFN-α (OIF; Otsuka Pharmaceutical Co., Ltd.) at a dose of 20,000 U/mouse or PBS (control) was intraperitoneally administered. After 24 h, 50 μg of Alexa Fluor 680-conjugated anti-FGFR1 mAb was intravenously administrated via the tail vein. The mice were then imaged under anesthesia using an IVIS LUMINA imaging system (Caliper Life Sciences, Hopkinton, MA, USA).

Supporting Information

Figure S1 Induction of *FGFR1* transcripts by IFN-α and IFN-β. HepG2 cells (1×10^6 cells) were subcutaneously xenografted into the backs of SCID mice. When the inoculated tumor had reached 10 mm in diameter, IFN-α or IFN-β was administered intraperitoneally or intravenously at a dose of 2000 U/mouse. Tumor tissues were then collected 0, 1, 3, 8, 24 and 48 h after administration. A, Time-course of FGFR1 and OAS1 (control) mRNA expression following administration of IFN-α. FGFR1 mRNA (blue line) was increased 3 h (151%), 8 h (202%) and 24 h (119%) after administration. OAS1 mRNA (red line) was increased 3 h (162%), 8 h (133%) and 24 h (150%) after administration. Shown are means of two replicates of the real-time RT-PCR. B, Time-course of FGFR1 and OAS1 mRNA expression after administration of IFN-β. FGFR1 mRNA (blue line) was increased 8 h (348%) and 24 h (337%) after administration, while OAS1 mRNA (red line) was increased 3 h (262%) and 8 h (511%) after administration. The levels of mRNA expression were normalized to that of GAPDH mRNA. The expression level at 0 h was taken as 100%.
(TIFF)

Figure S2 Evaluation of anti-FGFR1 monoclonal antibodies. A, Western blot analysis for FGFR1 in NIH3T3 cells stably transfected for FGFR1. The antibodies used are shown below the panel. B, Surface plasmon resonance analysis. The affinity of anti-FGFR1 mAb for FGFR1 was determined based on surface plasmon resonance. The extracellular domain of FGFR1, which was fused to the constant region of mouse IgG1, was covalently coupled to a CM-5 sensor chip at a density of 3400 response units. Binding kinetics were determined using two-fold serial dilutions of antibody at concentrations ranging from 200 to

12.5 nM in running buffer (PBS, pH 7.4, filtered and degassed). The regeneration procedure was carried using 15 μL of 3 M sodium thiocyanate. B, The apparent association and dissociation rate constants (ka1 (1/Ms) and kd1 (1/s)) and Kd values for A2C9-1 and A2D11-1.
(TIFF)

Figure S3 Histological analysis of human hepatic cancer cell-xenograft tumors. Hematoxylin and eosin (HE) staining of xenograft tumors from mice treated with PBMC only, IFN-α only, A2C9-1 only, IFN-α+A2C9-1 and IFN-α+A2C9-1+PBMC. Tumors were harvested 1 week after the final treatment. Note the marked infiltration by mononuclear lymphocytes of tumors from mice treated with IFN-α+A2C9-1+PBMC and the absence of infiltration of tumors from the other groups.
(TIFF)

Acknowledgments

The authors thank Dr. William F. Goldman for editing the manuscript.

Author Contributions

Conceived and designed the experiments: SS TI KI M. Tsujisaki YS. Performed the experiments: SS TI AO AT HT HS . Analyzed the data: H. Yasui H. Yamamoto HT M. Toyota. Contributed reagents/materials/analysis tools: TS YS AO MM . Wrote the paper: M. Toyota HS KI SS.

References

1. El-Serag HB, Rudolph KL (2007) Hepatocellular carcinoma: epidemiology and molecular carcinogenesis. Gastroenterology 132: 2557–2576.
2. El-Serag HB (2004) Hepatocellular carcinoma: recent trends in the United States. Gastroenterology 127: S27–34.
3. Cunningham D, Humblet Y, Siena S, Khayat D, Bleiberg H, et al. (2004) Cetuximab monotherapy and cetuximab plus irinotecan in irinotecan-refractory metastatic colorectal cancer. N Engl J Med 351: 337 345.
4. McLaughlin P, Grillo-Lopez AJ, Link BK, Levy R, Czuczman MS, et al. (1998) Rituximab chimeric anti-CD20 monoclonal antibody therapy for relapsed indolent lymphoma: half of patients respond to a four-dose treatment program. J Clin Oncol 16: 2825–2833.
5. Slamon DJ, Leyland-Jones B, Shak S, Fuchs H, Paton V, et al. (2001) Use of chemotherapy plus a monoclonal antibody against HER2 for metastatic breast cancer that overexpresses HER2. N Engl J Med 344: 783–792.
6. Tanaka S, Arii S (2009) Molecularly targeted therapy for hepatocellular carcinoma. Cancer Sci 100: 1 8.
7. Ku XM, Liao CG, Li Y, Yang XM, Yang B, et al. (2007) Epitope mapping of series of monoclonal antibodies against the hepatocellular carcinoma-associated antigen HAb18G/CD147. Scand J Immunol 65: 435–443.
8. Greiner JW, Guadagni F, Noguchi P, Pestka S, Colcher D, et al. (1987) Recombinant interferon enhances monoclonal antibody-targeting of carcinoma lesions in vivo. Science 235: 895–898.
9. Takahashi H, Okai Y, Paxton RJ, Hefta LJ, Shively JE (1993) Differential regulation of carcinoembryonic antigen and biliary glycoprotein by gamma-interferon. Cancer Res 53: 1612–1619.
10. Stark GR, Kerr IM, Williams BR, Silverman RH, Schreiber RD (1998) How cells respond to interferons. Annu Rev Biochem 67: 227–264.
11. Honda K, Takaoka A, Taniguchi T (2006) Type I interferon [corrected] gene induction by the interferon regulatory factor family of transcription factors. Immunity 25: 349–360.
12. Acevedo VD, Ittmann M, Spencer DM (2009) Paths of FGFR-driven tumorigenesis. Cell Cycle 8: 580–588.
13. Dvorak P, Hampl A (2005) Basic fibroblast growth factor and its receptors in human embryonic stem cells. Folia Histochem Cytobiol 43: 203–208.
14. Huang X, Yu C, Jin C, Kobayashi M, Bowles CA, et al. (2006) Ectopic activity of fibroblast growth factor receptor 1 in hepatocytes accelerates hepatocarcinogenesis by driving proliferation and vascular endothelial growth factor-induced angiogenesis. Cancer Res 66: 1481–1490.
15. Kan M, Wu X, Wang F, McKeehan WL (1999) Specificity for fibroblast growth factors determined by heparan sulfate in a binary complex with the receptor kinase. J Biol Chem 274: 15947–15952.
16. Hildebrandt MA, Gu J, Lin J, Ye Y, Tan W, et al. (2010) Hsa-miR-9 methylation status is associated with cancer development and metastatic recurrence in patients with clear cell renal cell carcinoma. Oncogene 29: 5724–5728.
17. Motoo Y, Sawabu N, Nakanuma Y (1991) Expression of epidermal growth factor and fibroblast growth factor in human hepatocellular carcinoma: an immunohistochemical study. Liver 11: 272–277.
18. Mise M, Arii S, Higashituji H, Furutani M, Niwano M, et al. (1996) Clinical significance of vascular endothelial growth factor and basic fibroblast growth factor gene expression in liver tumor. Hepatology 23: 455–464.
19. Hu Z, Evarts RP, Fujio K, Omori N, Omori M, et al. (1996) Expression of transforming growth factor alpha/epidermal growth factor receptor, hepatocyte growth factor/c-met and acidic fibroblast growth factor/fibroblast growth factor receptors during hepatocarcinogenesis. Carcinogenesis 17: 931–938.
20. Asada N, Tanaka Y, Hayashido Y, Toratani S, Kan M, et al. (2003) Expression of fibroblast growth factor receptor genes in human hepatoma-derived cell lines. In Vitro Cell Dev Biol Anim 39: 321–328.
21. Qu XJ, Yang JL, Russell PJ, Goldstein D (2004) Changes in epidermal growth factor receptor expression in human bladder cancer cell lines following interferon-alpha treatment. J Urol 172: 733–738.
22. Yang JL, Qu XJ, Russell PJ, Goldstein D (2004) Regulation of epidermal growth factor receptor in human colon cancer cell lines by interferon alpha. Gut 53: 123–129.
23. Platanias LC (2005) Mechanisms of type-I- and type-II-interferon-mediated signalling. Nat Rev Immunol 5: 375–386.
24. Darnell JE, Jr., Kerr IM, Stark GR (1994) Jak-STAT pathways and transcriptional activation in response to IFNs and other extracellular signaling proteins. Science 264: 1415–1421.
25. Weiner LM, Surana R, Wang S (2010) Monoclonal antibodies: versatile platforms for cancer immunotherapy. Nat Rev Immunol 10: 317–327.
26. Imai K, Takaoka A (2006) Comparing antibody and small-molecule therapies for cancer. Nat Rev Cancer 6: 714–727.
27. Harris M (2004) Monoclonal antibodies as therapeutic agents for cancer. Lancet Oncol 5: 292–302.
28. Kinebuchi M, Ide T, Lupin D, Tamatani T, Miyasaka M, et al. (1991) A novel cell surface antigen involved in thymocyte and thymic epithelial cell adhesion. J Immunol 146: 3721–3728.